ONLINE APPENDIX

ARTICLE TITLE:

Discovery of a giant chameleon-like lizard (*Anolis*) on Hispaniola and its significance to understanding replicated adaptive radiations

JOURNAL:

American Naturalist

AUTHORS:

D. Luke Mahler[1*], Shea M. Lambert[2], Anthony J. Geneva[3], Julienne Ng[4], S. Blair Hedges[5], Jonathan B. Losos[3], and Richard E. Glor[6]

AFFILIATIONS:

[1]Department of Ecology and Evolutionary Biology, University of Toronto, Toronto, ON M5S 3B2, Canada
[2]Department of Ecology and Evolutionary Biology, University of Arizona, Tucson, AZ 85721, USA
[3] Department of Organismic and Evolutionary Biology and Museum of Comparative Zoology, Harvard University, Cambridge, MA 02138, USA
[4]Department of Ecology and Evolutionary Biology, University of Colorado-Boulder, Boulder, CO 80309, USA
[5]Center for Biodiversity, Temple University, Philadelphia, PA 19122, USA
[6]Herpetology Division, Biodiversity Institute and Department of Ecology and Evolutionary Biology, University of Kansas, Lawrence, KS 66045, USA
*corresponding author; e-mail: luke.mahler@utoronto.ca

TABLE OF CONTENTS:

S1: EXPANDED SYSTEMATIC ACCOUNT OF *Anolis landestoyi* sp. nov.

(a) Field observations

15 observations of *A. landestoyi* have been made in the wild since 2007 (table S1), but specimens were not collected in all instances, and it is possible that some individuals were observed on more than one occasion. Six individuals have been collected, and three unique individuals have been observed since the last was collected, so a minimum of nine different individuals have been located in the wild. All have been located within 3 km of the type locality and were found within the boundaries of Reserva Biológica Loma Charco Azul. In the following description, each field observation is given a unique record number (note that some individual lizards may have two record numbers if they were observed more than once). For the six individuals collected as specimens, we also report field tag numbers and museum numbers (see also table S1). Note that there are two additional individuals of *A. landestoyi* that are known, but have never been observed in the field, as they were hatched in captivity. Information about those individuals is presented in the Reproduction section below, as well as in table S1.

Miguel Landestoy made the first definitive observation of this species on 21 May, 2007. That day, between 11:00-12:00 h, he located and was able to capture an adult male (MAL_DR2007_01), confirming it as an unknown species. On this occasion, Miguel Landestoy was observing a mated pair of Bay-breasted Cuckoos (*Coccyzus rufigularis*) with binoculars as part of a population viability survey, and these birds led him to the lizard. The birds had detected the anole on a nearby branch, and one of them briefly mobbed it. This lizard was cryptic both in pattern and in its movements, and Mr. Landestoy was only able to discern its presence by carefully scanning each nearby branch

with his binoculars. When he located it, the anole was clinging tightly to a vertical branch at a height of roughly 400 cm with its head facing the ground. Mr. Landestoy captured and briefly photographed the lizard, but the animal escaped while being photographed and Mr. Landestoy was unable to recapture it or locate another specimen. Mr. Landestoy showed a digital photograph of the head and anterior part of the body of this lizard to two of the authors (DLM, REG) during an August, 2008 field season. The authors were uncertain whether the animal was a new species, but no attempt was made to locate an additional specimen at that time.

On 22 March, 2010, Miguel Landestoy located and collected an adult female (MCZ R-188778; field tag Mahler 1838; MAL_DR2010_01) sleeping at night on a perch roughly 5.5 m high.

On 1 April, 2010, Miguel Landestoy and Luke Mahler collected a male (holotype MCZ R-188774; field tag Mahler 1864; DLM_DR2010b_02) and a female (MCZ R-188777; field tag Mahler 1861; DLM_DR2010b_01) at night. The male was located at 21:10 h sleeping with its head facing downward, clinging tightly to a diagonal branch covered in green lichen. It was perched at a height of 310 cm on a 1.6 cm diameter branch. The female was located at approximately 21:40 h perched head down on the underside of a diagonal branch (height = 306 cm, diameter = 2.5 cm). This animal was awake when located, possibly because it had recently begun to rain (this may also explain its position).

In early April 2010, Nicolas Corona located an adult male sleeping at night while guiding a birdwatching tour (MAL_DR2010_02). This lizard was photographed by his clients.

On 1 May, 2010, Miguel Landestoy, Tulio Mejia, and Yoel Hernandez located two adult male individuals before dawn and videotaped these animals in the wild intermittently over the course of four and a half hours in the morning. The larger of these animals (MAL_DR2010_03) was found sleeping roughly 450 cm high in a 600-700 cm tree. Over the course of the morning, this animal first remained fairly stationary near its nocturnal perch, but it eventually slowly climbed a neighboring tree, vanishing from sight near the top, at a height of roughly 900-1,000 cm. The smaller male (MAL_DR2010_04) was found sleeping roughly 500 cm high in an acacia tree that was approximately 700-800 cm in total height. That animal was videotaped for several periods from 6:00 – 10:30 h.

On 4 May, 2010, Miguel Landestoy located a large adult female (MAL_DR2010_05) sleeping head down on a vertical perch (~300 cm high) at night which he photographed in situ, but when he returned before dawn to observe its behavior, the animal had deserted its perch.

On 7 July, 2010, Miguel Landestoy collected an adult male (MCZ R-188776; field tag GLOR 07567; MAL_DR2010_06) and female (MCZ R-188779/MNHNSD 23.2979; field tag GLOR 07566; MAL_DR2010_07; deposited in the Colección de Reptiles, Museo Nacional de Historia Natural, Santo Domingo, República Dominicana) at night while on an ichthyology research trip with Arlen Marmolejo and Victor de la Rosa. The male was sleeping approximately 500 cm in an acacia tree on the side of a road, and the female was sleeping roughly 400-450 cm in a tree on the opposite side of the road. These individuals were housed together for several days in captivity, during which time they were observed mating (see next section for details).

On 22 January, 2011, Miguel Landestoy, Daniel Scantlebury, and Anthony Geneva collected a large adult male (MCZ R-188775; field tag GLOR 07803; MAL_DR2011_01) sleeping at night in a tree very close to where the specimens from 7 July, 2010 were collected.

On 21 May, 2011, while assisting biologist María Quírico with fieldwork in the region of the type locality of the new anole, Miguel Landestoy captured and photographed a large adult male (DLM_DR2011_11) and a juvenile female (MAL_DR2011_02) while they were sleeping. The adult male was kept in captivity for 21 days and was weighed and measured prior to release. The juvenile was photographed and released shortly after capture.

On 9 June, 2011, Miguel Landestoy, Luke Mahler, Martha Muñoz, and Maureen Stimola located a sleeping juvenile (DLM_DR2011_13) in the vicinity of the location of the individuals observed on 21 May, 2011. This animal was left undisturbed in the hopes of making behavioral observations in the morning, but it deserted its perch before dawn.

On 10 June, 2011 Miguel Landestoy, Luke Mahler, Martha Muñoz, Maureen Stimola, and Jorge Brocca located a juvenile male (DLM_DR2011_12) sleeping head down in hanging Spanish moss 430 cm above the ground. The next morning (11 June, 2011) this individual was videotaped from approximately 05:45-11:00 h for behavioral and habitat use data.

(b) Expanded description of the holotype

The holotype (MCZ R-188774) is an adult male with everted hemipenes (figures 2, S1, S3, S5). Compared to other *Anolis*, the tail (151 mm) is very short relative to the length of the body (SVL = 124 mm). The head is moderately elongated, but the snout is

not particularly attenuated. The body of this anole is slightly laterally compressed.

The anterior dorsal cranial scales are large, irregular, rugose, and pyramidal, producing a coarse, embossed texture (figures 2a, S1a,b). Blocky, enlarged scales with tall, blunt longitudinal ridges form pronounced canthal ridges that divide the highly rugose dorsal snout scales from the comparatively flatter loreal scales. Between the canthal ridges are two similarly composed longitudinal nasal ridges, and these have a shallow medial depression between them. The blocky scales of the dorsal snout surface give way posteriorly to slightly smaller and more pointed scales between the supraorbital semicircles, and eventually to granular scales in the temporal region. The parietal scale is larger than adjacent scales and is slightly longer than it is wide (figure S1b). The borders of the dorsal cranial scales (those that overlie the parietal, frontal, prefrontal, nasal, premaxilla, and maxilla bones) correspond closely with the texture of the underlying bone. These scales appear as though they contain osteoderms, but the bony structures that correspond with these scales are actually raised elaborations of the cranial periosteum (Etheridge and de Queiroz 1988; this feature is common to many iguanian lizards with enlarged bony cranial scales). The subocular scales are somewhat rugose and possess a single, modest, continuous keel. The loreals, supralabials, and sublabials are large, well differentiated, and rugose at a fine scale, but are flat in comparison with the dorsal cranial scales. The scales of the chin and eyelids are small, granular, and sometimes pointed, and are arranged loosely into longitudinal rows. The nasals exhibit the circumnasal condition, but nonetheless show anteroventral sutures. The mental scale is partially divided posteriorly. The temporal scales posterior to the parietal region are smooth, flat, relatively large, and irregular, as are the scales between the eye and the ear. Those behind the ear

opening are smaller and increasingly granular or bumpy, but still irregular. The ear opening is ovular, roughly twice as tall as it is wide, and has 2-3 enlarged scales along its dorsal margin that fold back into the auricular opening. It is roughly equal in size to the parietal scale (figures 2a, S1a,b).

We provide scale counts for the type series in table S2. The holotype has 7 scales across the snout between the 2nd canthals (counted from posterior to anterior), 6 postrostrals, 2 scales between the supraorbital semicircles, and 6 postmentals (not including a single tiny tubercle that abuts the central suture of the mental). On the left and right respectively (denoted in fractional notation), the holotype has 1/1 scales between the nasal and the rostral, 3/2 enlarged supraciliaries, 5/5 poorly defined loreal scale rows, 3/4 scales between the interparietal and the supraorbital semicircles, 0/0 scales between the suboculars and the supralabials, 9/10 supralabials from the rostral to directly beneath the eye, and 4/5 sublabials in contact with the infralabials (figure S1; table S2). Note that it is not possible to observe the fact that only 4 sublabials contact the infralabials on the animal's left side from figure S1c, as the scales that separate these rows posteriorly are obscured from view.

The dorsal body scales are primarily large, flat, and smooth, and circular or subrectangular in shape. They are distributed irregularly and are non-imbricate. Those dorsals within 4-6 rows of the dorsal midline are weakly unicarinate. A continuous nuchal and dorsal crest is composed of a single row of large, raised, leathery, triangular scales that begins just behind the posterior margin of the skull and continues to approximately 2 cm behind the posterior border of the pelvis. Initially nearly conical, these scales quickly become laterally compressed and more triangular, but they always

retain a distinct point. These enlarged scales are heterogeneous in size, with the largest scales spaced alternately or at every third scale. The skin flanking this crest is loose in comparison to the rest of the dorsum, and the large dorsal scales in this region are separated by slightly more interstitial skin. This corresponds to the ability of this species to voluntarily erect its crest to a height of several millimeters during displays. The ventral scales are weakly to strongly keeled, subimbricate, slightly mucronate, and more regularly distributed than the dorsal scales. The ventrals under the abdomen gradually decrease in size towards the ventral midline. The ventral midline is visible between the posterior margin of the dewlap and the pelvis as a distinct interruption of the ventral scale rows. For the skin covering the limbs, the situation is reversed in several regards. On both the fore- and hindlimbs, nearly all dorsal scales are keeled, imbricate, and arranged into regular diagonal rows (the dorsal digital scales are imbricate and multicarinate), while the ventral scales are non-imbricate (or very mildly imbricate), circular, and less regularly arranged. Ventral scales are larger under the radius and ulna than under the humerus or the sole of the forefoot, and are likewise larger under the tibia and fibula than under the femur or the sole of the hindfoot. Digits of both forefeet and hindfeet exhibit well-developed adhesive subdigital toepads. The fourth digit of the left hindfoot has 43 enlarged subdigital scales, including 27 under the second phalanx that are adorned with setae (45 and 28 on the right; figure S3d). The fourth digit of the left forefoot has 28 enlarged subdigital scales (or in 2 cases, pairs of scales), including 19 under the second phalanx that are adorned with setae (28 and 19 on the right forefoot). Claws are tall and robust proximally and recurved distally (some claws of the preserved holotype became slightly worn in captivity, but their original shape is evident in photographs; figure S3d).

The cloaca forms an anteriorly concave semicircle (figure 2c). The scales anterior to the cloaca are granular and round or slightly mucronate. Just posterior of the cloaca, the scales are immediately small and granular, and then slightly larger and flatter. Three millimeters posterior of the cloaca, these scales are abruptly interrupted by a pair of large subrectangular postanal scales. Caudal to the postanals, the scales become large, smooth, and round, but within 20 mm, they transition into regular rows of flat, imbricate, keeled scales (both dorsally and ventrally), which continue to the tip of the tail. The tail tip is blunt, and marked by an expanded "tuft" of scales (figure 2b,c). The tail is strongly laterally compressed, and has a distinct crest anteriorly (continuous with the dorsal crest) that grades into serrations posteriorly.

The hemipenes are large, fairly stout, weakly bilobed and symmetrical (figure S5). In the holotype, the left hemipenis is more fully everted than the right hemipenis, and on the left, the anterior lobe is completely everted and the posterior lobe is nearly completely everted. As preserved, the left hemipenis extends to the tenth caudal scale row posterior to the enlarged postanal scales[1]. The surface of the pedicel is naked basally and covered in transverse ridges where it meets the apex. These ridges, or flounces, *sensu* Dowling and Savage (1960), also cover the basal region of the apical lobes. The lobes, which are weakly differentiated, are covered in small calyces, which become smaller distally. On the sulcate side (figure S5a), the sulcus spermaticus is deep with well-developed sulcal lips. The sulcus spermaticus extends to the crotch of the lobes and opens into a concave, ovular nude patch that covers most of the surface of the lobes on the sulcate side. The

[1] During a recorded mating event, a different individual (MCZ R-188776; see below) was observed to extend the hemipenis further – to a distance nearly equal to the length of the thigh. This difference may be attributed to the fact that we did not sever the *m. retractor penis magnus* muscle as we prepared the holotype specimen.

oval nude area has a fold that is perpendicular to the sulcus spermaticus and that divides the oval along its long axis (together, the sulcus spermaticus and this folded nude patch form a "T"). The nude area is bordered by roughly four to seven ridges, and which become retiform distally, eventually grading into fine calyces. On the asulcate side (figure S5b), the transverse flounces just basal to the two lobes grade apically into deep reticulated folds in the groove formed by the junction of the two lobes. This ornamented crease extends nearly to the nude patch of the sulcate side, but terminates just prior in a shallow pocket. From this medial crease, these folds quickly grade distally into calyces, which become increasingly smaller toward the tips of the lobes.

Dorsal pattern and coloration is lichenate in life (figure 2b), similar to anoles such as *A. insolitus*, *A valencienni*, *A. sheplani*, and *A. proboscis* (Webster 1969; Williams and Rand 1969; Schwartz 1974; Hicks and Trivers 1983; Losos et al. 2012). The dorsal surfaces are predominantly greenish-grey and light brown, mottled with irregularly shaped black and brown blotches and speckles. The dorsal surface of the head is light brown with a charcoal-colored "W" crossing the snout, and a darker "X" between the orbits (roughly outlining the supraorbital semicircles). The skin directly above the eyes is cream-colored with irregular dark streaks. Behind the head, a series of large, irregular, brown vertebral saddles extends from the pectoral region to the end of the tail (three large blotches between the girdles, one X-shaped saddle over the pelvis, and nine blotches on the tail). The hindlimbs exhibit a similar pattern – with the hindlimb flexed such that the thigh and calf are adpressed, one large, continuous dark band traverses both the middle of the thigh and the calf just above the ankle, while another crosses both the thigh and the calf just proximal to the knee. These bands disrupt the outline of the hind leg. The upper

flanks are greenish-grey fading to greyish-white ventrally. This base pattern is overlaid by three crude longitudinal rows of charcoal-colored X-shaped markings, which appear to correspond very loosely to the vertebral saddles and ventral reticulations and form an oblique banding pattern. The side of the head is similarly patterned – greenish-grey with irregular black or charcoal-colored reticulations. When the eye is closed, the most prominent of these dark streaks crosses the eyelid and widens near the corner of the mouth, breaking the outline of the eye (figures 2a, S3b). This streak extends ventrally to meet the innermost and most prominent of several concentric black or charcoal-colored rings on the dewlap (figure S3b; also evident in paratypes in figures S2a, S4b). A dark, distinct nuchal ocellus approximately the same size as the eye sits between the shoulder and the posterior corner of the lower jaw.

Ventral surfaces are white with charcoal reticulations (figure 2c). Under the body, the reticulations are arranged very unevenly into approximately five transverse bands, which are loosely continuous with the dark dorsal saddles; the left and right halves of each band meet unevenly at the ventral midline, which, between the base of the dewlap and the pelvic region, is marked by a crease disrupting the ventral scale rows (figure 2c). The chin is also traversed by reticulated bands, although these become very faint and speckled anteriorly. One charcoal-colored band, located just behind the level of the eyes, is particularly bold, although it is interrupted medially by the white scales that form the edge of the dewlap. The gular skin on either side of the ventral midline, and posterior to the first third of the head, is elaborately bunched and wrinkled when the dewlap is not in extension, giving the throat a somewhat frilled appearance. The skin in between these folds is bluish, revealing the color of the dewlap (figure 2c). The undersurfaces of the

limbs are evenly reticulated, although these reticulations give way to sparse speckling on the undersurfaces of the feet. The ventral surface of the tail has ten evenly spaced ocelli between the cloaca and the tail tip, each with an irregular dark border and lighter inner coloration (white to grey). The spaces between these ocelli are broken by dark, thin partial bands (figure 2c).

The iris exhibits a starburst pattern with a thin cream-colored ring immediately surrounding the pupil that gives way to a distally radiating pattern of dark brown streaks on a cream-colored background (figure S3a).

The dewlap, which is moderately large, has a base color of sky blue centrally, and this color becomes fainter towards the distal margin of the dewlap (figure 2a). This bluish coloration is absent from the anterior corner of the dewlap and is very faint in the posterior corner. The dewlap is longitudinally striated with indistinctly defined rows of white or greyish-white enlarged scales (seven full or partial rows at the deepest point of the dewlap). The edge of the dewlap is colored white with very light brown speckling. In addition to the bluish base color and white longitudinal striations, the dewlap exhibits a pattern of dark, reticulated striations that largely alternate with the white striations, but occasionally cross them (figure 2a). These dark markings vary in visibility with the temperament of the animal (as does the bluish color of the dewlap). Sometimes these dark reticulations are most apparent in the posterior and anterior corners of the dewlap and are expressed very faintly towards the dewlap's center (figure 2a). However the animal is capable of voluntarily darkening the dewlap such that these dark reticulations are prominent across the entire dewlap, effectively obscuring the bluish coloration, but not the white longitudinal banding pattern (in fact, the latter becomes more striking when

the dewlap is darkened) (figure S3b). In addition, the dewlap exhibits several black or charcoal-colored concentric semicircular rings, centered around the nuchal ocellus. Similar to the black reticulations, these rings are poorly defined, but they differ in that they disrupt the white longitudinal banding pattern (figure S3b; also visible in paratypes in figures S2a, S4b). The visibility of these rings also varies with temperament (figure 2a versus figure S3b), and the innermost ring is the thickest and most well defined.

The tongue and lining of the mouth is white with a tinge of pink, and the skin from the corner of the mouth (scale-less skin generally only visible when the mouth is open) is light bluish-grey in color (figure S3c).

In preservative, the bluish color of the dewlap and the greenish-grey color of certain scales fade to greyish-white, but other aspects of pattern and color remain unchanged.

(c) Morphological variation within the type series

The features described for the holotype, both in pattern, gross morphology, and scalation, are also representative of the two adult males in the paratype series. The three adult female paratypes are similar in most regards, but exhibit more modestly developed scales on the dorsal surface of the cranium, a slightly smaller dewlap, and lack enlarged postanal scales (postanal scalation is much more uniform in females) (figure S2). Males and females appear to be similar in scalation, body size, and in most other morphological dimensions, although females have larger abdomens (tables S1–2, S4, figure S2).

Juveniles are similar to adults but differ in that they have proportionally shorter snouts and taller skulls (figure S4). Juvenile dorsal cranial scales are unicarinate, but relatively flat and smooth compared to adults, suggesting that the osseous sculpturing associated with the large rugose cranial scales develops with maturity. The parietal scale

is more distinct in juveniles. Like other Hispaniolan giant anoles, *A. landestoyi* individuals of both sexes hatch with fully developed, functional dewlaps (figure S4b).

Juveniles may be distinguished from adults of smaller species of cryptic Hispaniolan *Anolis* by cranial and body shape differences; in juvenile *A. landestoyi*, the body is stout for its size and the head is large, with a distinctive short snout (figure S4). Although juveniles of the new species resemble adult Hispaniolan twig anoles (e.g., *A. darlingtoni*, *A. insolitus*) in pattern and limb and tail dimensions, the latter are smaller and have considerably more gracile bodies and elongate heads. *Anolis landestoyi* juveniles also differ from *A. darlingtoni* and *A. insolitus* by the presence of enlarged anterior supraciliary scales, greater numbers of scales between the supraorbital semicircle scale rows and between the pineal scale and the supraorbital semicircles, keeled ventral scales, and the presence of a middorsal crest (table S1).

(d) Distribution and habitat

All specimens were located within the Reserva Biológica Loma Charco Azul or its immediate environs (Independencia Province, Dominican Republic; figures 2d, S6a,b) and were found at 455-526 m elevation. Although the southwestern boundary of Loma Charco Azul extends to the border of Haiti, this species has thus far only been observed in the Dominican Republic. The habitat at Loma Charco Azul ranges from lowland spiny shrub forest and semi-deciduous dry forest in the north of the reserve to transitional and montane wet forest in southern parts of the reserve, which contain foothills of the Sierra de Bahoruco. The new species has only been observed in the mid-elevation transition zone between the dry forest and broadleaved upland rainforest (figure S6a,b). At collection sites, representative vegetation includes several mimosoid trees (e.g., *Acacia*,

Calliandra), gumbo-limbo (*Bursera simaruba*), roughbark lignum-vitae (*Guaiacum officinale*), mesquite (*Prosopis juliflora)*, West Indian boxwood (*Phyllostylon brasiliensis*), wine palm (*Pseudophoenix vinifera*), and cactus (e.g., *Harrisia*) (Perdomo et al. 2010). Spanish moss (*Tillandsia*) and lichens are common epiphytes at the type locality. Reserva Biológica Loma Charco Azul contains critical habitat for several endangered bird species including the Bay-breasted Cuckoo (*Coccyzus rufigularis*), La Selle Thrush (*Turdus swalesi*), and Hispaniolan Crossbill (*Loxia megaplaga*), as well as other endangered Hispaniolan endemics such as the solenodon (*Solenodon paradoxus*) and Ricord's Iguana (*Cyclura ricordii*).

(e) Microhabitat use and behavior

Four individuals of *A. landestoyi* have been observed in the wild during the day (we refer to each by its field observation number; see table S1). The first (MAL_DR2007_01) was the individual discovered by Miguel Landestoy while observing a pair of Bay-breasted Cuckoos (*Coccyzus rufigularis*). In 2010 and 2011, three additional animals (MAL_DR2010_03, MAL_DR2010_04, DLM_DR2011_12) were located at night and videotaped undisturbed after they awoke the next morning. In this paper, we provide a brief qualitative description of the habitat use and behaviors of the animals we observed, and we refer interested readers to future quantitative work on the subject, currently in preparation. To supplement our *in situ* observations of behavior, we observed several animals in captivity, mindful that such observations may not reflect natural behavior.

During observation periods, individual *A. landestoyi* were stationary for the majority of the time. When individuals were moving, they moved primarily by crawling or walking, although occasionally individuals were seen to move quickly. Both when

perching and when moving, *A. landestoyi* primarily utilized perches of small diameter, often comparable in girth to the lizard itself, and frequently narrower. Individuals were never observed to descend to the ground and typically perched at heights of several meters or higher. A large male (MAL_DR2010_03) that we observed slowly ascended from its night perch (~450 cm) to the upper branches of a ~1,000 cm tree over the roughly four hour period during which we made observations. During this period of movement, this male navigated a complex and tangled network of thin branches. In general, it did so relatively slowly and when moving from branch to branch, it actively changed the orientation of its tail, at some points elevating the organ as a counterbalance and at others placing it in contact with branches for stability.

Two individuals of *A. landestoyi* were observed using their dewlaps to display in the wild. The small male observed on 1 May 2010 (MAL_DR2010_04) displayed a single time for four seconds. It abruptly elevated the front of its body by extending its front legs and simultaneously extended its dewlap. This male only held the dewlap out for slightly more than one second, and while retracting the dewlap, briefly pushed it nearly fully out again before retracting completely and lowering the head. The juvenile male observed on 11 June 2011 (DLM_DR2011_12) displayed several times for longer periods of time. Its first display, observed at 06:08 h, was likely a broadcast display. This animal raised its head and extended its dewlap as described above, but held the dewlap out for 62 seconds. Over this period, it relaxed the dewlap very slowly to about half of the full extension and at 62 seconds, it extended the dewlap fully three times in rapid succession, holding it out after the third extension. It held the dewlap extended for about 30 seconds and then repeated the same three-pulse bout of extensions, holding the dewlap

out for about 40 seconds.

Anolis landestoyi may also erect a prominent nuchal and dorsal crest as a signal. This crest is raised via vascular swelling of a ridge of dorsal skin (i.e., it is not bony nor is it composed of scales). The crest may increase the apparent depth of the animal by 50% (measured at the pectoral girdle) when viewed laterally. We have only seen this crest fully raised during observations of a single adult male (MAL_DR2010_03; filmed 1 May, 2010) and we have been unable to induce this behavior in captive animals. Nonetheless, the dorsal skin involved in raising the crest is distinct and it is present in all specimens we have examined (including males, females, and juveniles). We have not yet observed this species engage in intraspecific or interspecific interactions with other lizards in the wild.

(f) Reproduction

An adult male (MCZ R-188776) and an adult female (MCZ R-188779/MNHNSD 23.2979) briefly housed together in captivity were observed to mate on 11 July 2010. When discovered, the male had already climbed onto the back of the female and it proceeded to bite and grip the female's nuchal skin with the front, right side of its mouth. The male remained stationary for 64 seconds and while still biting the nuchal skin of the female he quickly shifted his body to her right side, lifted the base of her tail with his own tail, and proceeded to copulate using his left hemipenis. The female bobbed her head rapidly seven times immediately thereafter, and the pair mated in this position for over 14 minutes before the female broke free from the grip of the male and ran to the other side of the terrarium. We were unable to induce mating behavior or any other interactions between another male-female pair in captivity (MCZ R-188774 and MCZ R-188777) despite repeated attempts in late October 2010 and early July 2011. With this latter pair,

the male darkened and remained motionless each time the female was introduced to his cage, and efforts to let the male become accustomed to the female were unsuccessful.

Prior to being introduced to a male in captivity, the aforementioned captive female (MCZ R-188777) laid six eggs that were discovered on 20 October, 2010. Two of these eggs were viable, and both were buried or partially buried in the soil of a pot in the female's enclosure. Two additional eggs were either buried or partially buried, but were completely desiccated upon discovery and were preserved. Finally, two eggs were not buried, and these were inviable. We successfully incubated the two viable eggs, obtaining healthy hatchlings (MCZ R-188781, MCZ R-188780; figure S4). The first egg to hatch was inferred to have been laid in September, 2010, and hatched on 21 October, 2010. That egg measured 25 mm in length and 17 mm in diameter upon discovery, but was not weighed prior to hatching (which occurred the next day). The female hatchling (MCZ R-188781; Mahler 1862) weighed 2.0 g, and the empty eggshell weighed 0.4 g (both hatchling and eggshell are shown in figure S4).

The second viable egg weighed 2.2 g and measured 21.34 mm by 14.40 mm on 21 October, 2010 (one day after discovery). This egg produced a male hatchling on 6 December, 2010 (MCZ R-188780; Mahler 1863) which weighed 2.1 g (empty eggshell mass = 0.3 g). SVL and tail length measurements for both hatchlings are reported in table S1.

Because the mother was captured on 1 April, 2010 and housed in isolation until October, 2010, we infer that *A. landestoyi* females may store viable sperm for a period of at least five months. We also note that the younger hatchling (MCZ R-188780, a male) grew considerably faster than its slightly older sibling (MCZ R-188781, a female),

despite the fact that they were housed separately and fed according to the same routine (compare final sizes in table S1).

(g) Diet

To obtain a preliminary indication of diet, we flushed the stomachs of two individuals of *A. landestoyi* immediately upon capture (MCZ R-188774, MCZ R-188777, both on 1 April, 2010), and we collected feces from these same individuals in captivity for a period of one week. Stomach contents and feces contained the remains of a taxonomically broad sample of arthropods, including orthopterans, coleopterans, hemipterans, mantids, and arachnids, suggesting that the new species is a generalist insectivore rather than a specialist on any particular prey type. Both large and small arthropods were consumed, as has been reported for the Hispaniolan giant anole *A. barahonae* (Bowersox et al. 1994; Henderson and Powell 2009).

S2: SUPPLEMENTAL MATERIALS AND METHODS

(a) Specimen collection and preservation

We located lizard species from the Hispaniolan giant *Anolis* clade during visual searches, which we conducted predominantly at night with the aid of bright, battery-powered lights. We preserved specimens in the field using 10% buffered formalin or 95% ethanol, or in the laboratory using 95% ethanol. Prior to specimen preservation, we preserved tissue samples (from the liver, a muscle, or both) in ~100% ethanol. Once specimens were preserved, we transferred them to jars filled with 70% ethanol for long-term storage. Specimens are reported in tables S1 and S7.

(b) Phylogenetic analyses

To assess the phylogenetic affinities of *A. landestoyi*, we conducted several

analyses at both broad and fine phylogenetic scales within *Anolis*. Because many details differ among analyses, we outline them comparatively in table S8.

(i) Taxon sampling

We obtained tissue samples from three individuals of *A. landestoyi* from the type locality (MCZ R-188776, MCZ R-188778, MCZ R-188779/MNHNSD 23.2979). To infer the phylogenetic position of *A. landestoyi* within *Anolis*, we analyzed *A. landestoyi* sequence data with sequences from a phylogenetically diverse set of congeners (95 *Anolis* species, including *A. landestoyi*; 1 individual per species) as well as two outgroup taxa (*Leiocephalus* and *Polychrus*).

To further investigate the phylogenetic position of *A. landestoyi* within the clade containing the Hispaniolan giant anoles, we obtained tissue samples from a total of 62 individuals of the three previously described species assigned to the *ricordii* clade, sampled from 25 localities in the Dominican Republic: *A. baleatus* (N = 42, 16 localities), *A. barahonae* (N = 7, 4 localities), and *A. ricordii* (N = 13, 5 localities) (figure 2d). Our sample of *A. ricordii* included two localities from the Sierra de Bahoruco in close proximity (2-3 km) to the type locality for *A. landestoyi*. Voucher specimen data for newly collected materials are presented in tables S1 and S7, and a spreadsheet containing voucher information, locality information, and GenBank numbers for all sequences used in this study may be found on Dryad (http://dx.doi.org/10.5061/dryad.sf540) (Mahler et al. 2016).

(ii) DNA sequencing

We extracted genomic DNA from ethanol-preserved liver tissue using a Wizard® SV Genomic DNA Purification System kit following standard protocols. We used

previously developed PCR primers to amplify nine nuclear loci (RAG1, ROD, R35, BDNF, NT3, B108, B120, B127, and GJA1) and one mitochondrial gene (ND2) (table S9). Reactions totaled ~25 μl with 11.4 μl dH_2O, 2.5 μl each of forward and reverse primers at 2 μM concentration; 2.5 μl 10X Taq reaction Buffer (Mg++ free); 2.5 μl $MgSO_4$ (20 μM); 2.5ul dNTP mix (5 μM); 0.125 μl DNA Taq Polymerase (5 μ/μl); and 1-2 μl of genomic template DNA. We obtained dNTPs, Taq, and 10X buffer from Bio Basic Inc. (Markham, ON, Canada). We conducted PCR using Eppendorf Mastercycler ep gradient S thermocyclers with general reaction conditions as follows: 94°C for 120 seconds followed by 30-35 cycles of 94°C for 35 seconds, 52-66°C for 35 seconds, and 72°C for 90 seconds. One locus (RAG1) was amplified with a touchdown protocol as follows: 94°C for 300 seconds followed by 2 cycles each of 94°C for 30 seconds, 60 seconds with an initial annealing temperature of 62°C that decreased between cycles in increments of 2°C down to 54°C, 72°C for 90 seconds, followed by 30 cycles with an annealing temperature of 52°C. Beckman Coulter Genetics carried out PCR purification using SPRI technology and DNA sequencing in both directions using the same primers used amplification and the Big Dye Terminator v3.1 system on an ABI PRISM 3730xl capillary sequence analyzing system.

(iii) Sequence data and alignment

We edited and assembled sequences in Geneious v5.3 (Drummond et al. 2010). Because indels were rare, alignments were conducted primarily by eye. We confirmed sequence identity using NCBI BLAST for the five exons and ROD, and with BLAT searches of the *Anolis carolinensis* genome using the UCSC genome browser for three primers that were developed as part of the *Anolis* genome project (table S9; Alföldi et al.

2011). Our aligned mitochondrial data set consists of 1036 base pairs with 92.4% completeness and 512 variable characters (339 parsimony-informative). The aligned concatenated nuclear data set consists of 5564 base pairs with 96.0% completeness and 474 variable characters (149 parsimony-informative).

***(iv) Analyses of* A. landestoyi's *position in* Anolis**

With the goal of determining *A. landestoyi*'s phylogenetic position in *Anolis* we analyzed a data set including five nuclear loci (BDNF, GJA, NT3, RAG1, R35) for a phylogenetically diverse sample of 95 anole species (72 from the Greater Antilles), which included one of the paratypes of *A. landestoyi* (MCZ R-188775) and a single individual for each other species.

We estimated phylogenies using Bayesian methods in MrBayes v3.1.2 (Huelsenbeck and Ronquist 2001). We also used the consensus tree from the posterior distribution of this analysis as a starting tree for a BEAST (Drummond and Rambaut 2007) analysis in which we estimated both the topology and relative timing of anole diversification for subsequent comparative analyses.

We first used the Metropolis-coupled Markov Chain Monte Carlo (MCMCMC) method implemented by MrBayes to infer phylogenetic relationships within *Anolis*. In preliminary analyses, we optimized several parameters, including models of molecular evolution, partitioning strategies, temperature for heating of Metropolis-coupled chains, and chain length, as follows. We evaluated alternative partitioning strategies by comparing Bayes factors calculated from harmonic mean likelihood scores (Brandley et al. 2005). These scores were obtained using the sump command in MrBayes. Bayes factors significantly favored the most highly partitioned strategy we tested, in which each

protein-coding region was partitioned into three codon positions, plus one partition per intronic region (15 partitions in total for the nDNA analyses). We selected models of molecular evolution for each partition by comparing Akaike information criterion (AIC) scores of a wide range of models for DNA sequence evolution in jModelTest (Posada 2008) (table S10). Each MCMCMC analysis consisted of two independent runs with one cold chain and three incrementally heated chains per run, and we used MrBayes default settings for all parameters not otherwise specified. We performed preliminary analyses to identity 0.02 as the optimal heating parameter to provide levels of chain mixing between 20-80%. The final analysis was run for 100 million generations, with a sample frequency of one sample per 10,000.

We evaluated convergence of Bayesian analyses using several strategies. Using Tracer v1.4 (Rambaut and Drummond 2007), we examined time-series plots of -lnL and other model parameters for stationarity. Using the web utility Are We There Yet? (AWTY; Nylander et al. 2008), we examined the cumulative posterior probabilities of tree bipartitions for stationarity at evenly spaced increments of the MCMCMC analyses using the "cumulative" utility, and compared bipartition posterior probabilities between independent analyses with the "compare" utility. We defined burn-in as the point at which posterior probabilities reached a stable value, a point that varied among runs and data sets. After assessing convergence and removing burn-in topologies, we generated a consensus phylogram using the sumt command in MrBayes.

Next, we conducted a Bayesian uncorrelated relaxed clock analysis in BEAST (Drummond and Rambaut 2007) to simultaneously estimate the topology and relative timing of the anole diversification, using the MrBayes consensus tree as the starting tree.

For these analyses, we constrained the monophyly of *Anolis* and set the root age to a uniform distribution from 95 to 105 million years. We chose this range arbitrarily for the purposes of estimating relative divergence times from molecular data, but with no interest in estimating the absolute timing of Greater Antillean anole diversification (see Losos (2009) for discussion of several challenges to estimating the absolute timing of anole diversification). We used a Yule speciation topology prior as relationships among the taxa are interspecific. We performed these analyses for 100 million generations, sampling trees at a frequency of one per 1,000. We assessed convergence and concordance among analyses using Tracer and AWTY, as described for the MrBayes analyses above. We combined the results of three independent runs using the LogCombiner utility included with BEAST (Drummond and Rambaut 2007). Before combining the posterior samples, we thinned the sampling of each run to once every 25,000 generations and discarded the first 50 million generations as burn-in. We calculated the maximum clade credibility (MCC) chronogram with median node heights for the combined posterior sample (N = 6,003 trees) using the TreeAnnotator utility included in BEAST (Drummond and Rambaut 2007). We conducted all phylogenetic comparative analyses using this MCC chronogram.

(v) Analyses of* A. landestoyi's *position within the* ricordii *clade

After our genus-wide analyses placed *A. landestoyi* with the three Hispaniolan crown-giant anole species comprising the *ricordii* clade with strong support, we conducted more intensive molecular analyses of this group using broad taxonomic and geographic sampling (table S7, figure 2d). We obtained sequence data from 65 individuals (including three *A. landestoyi*) for one mitochondrial gene and nine nuclear

genes (tables S1, S7). We inferred the phylogenetic relationships of these individuals using two gene-tree/species-tree reconciliation methods of phylogenetic inference: *BEAST (Heled and Drummond 2010), and BUCKy (Ané et al. 2007; Larget et al. 2010). We also estimated phylogenetic trees separately for individual loci, concatenated nDNA, and concatenated nDNA plus mtDNA using standard Bayesian phylogenetic methods in MrBayes. All of these analyses are described in detail below.

- Species-tree analyses

Since introgressive hybridization, incomplete lineage sorting, and other processes can lead to discordance among gene-trees and between gene-trees and species-trees (Maddison 1997), we employed two methods for phylogeny estimation via gene-tree/species-tree reconciliation. Species-tree estimation algorithms make different assumptions about the underlying causes of gene-tree/species-tree discordance, and their performance varies among data sets (Chung and Ané 2011; Leaché and Rannala 2011). We used two Bayesian methods that may be expected to perform well under different circumstances: *BEAST v1.6.2 (Heled and Drummond 2010) and BUCKy v1.4.0 (Ané et al. 2007; Larget et al. 2010). For these methods, we analyzed nDNA + mtDNA data sets including all 65 individuals.

*BEAST co-estimates gene-trees and species-trees directly from multilocus sequence data in a hierarchical Bayesian framework using a multi-species coalescent model (Heled and Drummond 2010). This approach assumes a strictly bifurcating history of species divergence, and all gene-tree/species-tree incongruence is attributed to incomplete lineage sorting. We ran four independent *BEAST analyses of 100 million generations with a sample frequency of 2,000 for nDNA + mtDNA data sets. For

BEAST analyses, we tested models of molecular evolution for each gene separately using jModelTest (Table S10), and linked tree models within genes. We partitioned sequences and selected models of molecular evolution in the same manner as described for the MrBayes analyses above. We used a Yule process species-tree as the topology prior. We specified the ploidy type of each nuclear gene as "autosomal nuclear" and of ND2 as "mitochondrial." Prior to each analysis, we used likelihood ratio tests to evaluate a molecular clock hypothesis for each gene alignment, based on likelihood scores from maximum likelihood reconstruction implemented in PAUP v4.0b10 (Swofford 2003). For ND2 and ROD gene alignments, the molecular clock hypothesis was rejected, so we used an uncorrelated lognormal relaxed clock prior with an initial value of 1 and a uniform distribution from 0-100. For all other genes, we employed strict clock estimates (over a uniform distribution from 0-100) relative to a fixed rate of 1 for one gene (B108). We left all other parameters at default settings. We assessed convergence using Tracer and generated MCC trees using TreeAnnotator as described above.

BUCKy uses Bayesian concordance analysis (Ané et al. 2007) to estimate a concordance tree from a set of previously estimated gene-tree topologies. Because BUCKy does not assume a particular source of gene-tree/species-tree incongruence (Chung and Ané 2011), other potential causes of incongruence (e.g., horizontal gene transfer) can be accommodated. We conducted BUCKy analyses using individual gene-tree topologies (9 nDNA, 1 mtDNA) estimated with MrBayes (see below). Using the pruning table function, we ran 100 replicate analyses, each with a single randomly selected exemplar of each species. Each MCMCMC analysis consisted of four independent runs with four chains (one cold, three heated), 150,000 updates, and a

sample frequency of one per 1,000. We repeated this process setting the α discordance prior to values of 0.1, 1.0, and 10.0 (results did not differ, and we present results obtained with α = 1.0). We summarized the resulting sets of primary concordance trees using the "consensus" function in the R package APE (Paradis 2004).

- Bayesian phylogenetic analyses of individual and concatenated data sets

We conducted Bayesian phylogenetic analyses on (1) each gene individually, as well as on concatenated data sets comprising (2) all nuclear loci and (3) nuclear loci plus the mitochondrial locus ND2. For these analyses, we chose not to evaluate separate models of molecular evolution for codon position partitions within protein-coding genes, and instead applied the favored model estimated for each gene (see above) to codon partitions within each gene (Table S10). We took this approach because the codon partitions contained, at maximum, a few hundred characters, and simulations have shown that this may lead to biased selection of overly simplistic models of sequence evolution, particularly when the number of taxa is low (Posada and Crandall 2001). For the estimation of individual gene trees, we first merged identical sequences using MacClade (Maddison and Maddison 2005), and then conducted phylogenetic analyses using MrBayes (Huelsenbeck and Ronquist 2001). For these analyses, we used the protocols described above for estimating our BEAST starting tree, modified slightly to accommodate these data sets. We optimized the temperatures of incrementally heated chains to provide levels of chain mixing between 20-80%. Temperatures for these analyses ranged from 0.02–0.08, depending on the data set being analyzed. These analyses ranged from 20-25 million generations for individual loci and 100-282 million generations for concatenated analyses, with a sample frequency of one sample per

10,000.

We conducted all analyses on the BlueHive High Performance Computing cluster at the University of Rochester Center for Research Computing (https://www.rochester.edu/its/web/wiki/crc/).

(c) Ecomorphological analyses

To quantify the position of *A. landestoyi* in a morphological space composed of ecologically relevant traits, we measured 11 continuous variables for three adult males using digital calipers. These traits include body size (SVL), tail length, the number of subdigital adhesive lamellae in the toepads, and several measurements of the limb elements (table S11); these traits correspond to variables measured in previous studies of ecomorphological matching in anoles, which have been restricted to males (Losos et al. 1998; Beuttell and Losos 1999). We natural log-transformed and averaged individual trait values and then combined these species values with matching measurements (all taken by same individual [DLM]) for 71 other Greater Antillean anole species from the data set of Mahler et al. (2010). From this data set, we obtained independent size and shape axes using phylogenetic regression and phylogenetic principal component analysis (pPCA) on a covariance matrix of body size and shape residuals (Revell 2009); these analyses relied on the Bayesian MCC chronogram described previously; tables S11–12). We retained the first four PC axes based on examination of a scree plot, and these axes explain 94% of the variation in our data set. pPC 1 correlates strongly and positively with limb element lengths and tail length; pPC 2 correlates positively with SVL; pPC 3 correlates negatively with toepad lamella number, humerus length, and radius length, and positively with tail length; and pPC 4 correlates positively with toepad lamella number (tables S11–12). We

note that for two species included in our phylogenetic trees, we did not have suitable trait data for that species, but did have trait data for a very similar close relative. Thus, for our comparative analyses, measurements of *A. guazuma* correspond to *A. garridoi* in the phylogeny, and measurements of *A. centralis* correspond to *A. terueli* in the phylogeny.

We determined which Greater Antillean species are most similar to *A. landestoyi* by calculating their pairwise Euclidean distances (ED) in the four-dimensional morphological space described above. We then tested whether a group containing *A. landestoyi* and members of the Cuban *chamaeleonides* clade was as distinct in morphological space as groups that represent the six traditional *Anolis* "ecomorph" classes (sensu Williams 1972; Williams 1983; Losos 2009). We conducted a 7-category linear discriminant analysis (LDA) on traditional ecomorph class for the four cryptic giants in our sample (*A. landestoyi*, *A. chamaeleonides*, *A. guamuhaya*, *A. porcus*) plus all species in our Greater Antillean data set that have previously been assigned to one of the six traditional ecomorph classes (Williams 1972; Williams 1983; Losos 2009).

S3: SUPPLEMENTAL TABLES

Table S1. Individuals of *Anolis landestoyi* sp. nov. observed, collected, or reared during this study. Snout-to-vent length (SVL) and tail length measurements taken from preserved specimens unless animal was released, in which case the live animal was measured prior to release. Mass measured from live specimens just prior to preservation or release. Some additional length and mass measurements from life are provided in notes. Field tag numbers correspond to tip labels in the figures depicting the *ricordii* clade phylogenetic results. A dash indicates missing information.

Field Obs. Number	Field Tag Number	Museum Number	Date Observed or Collected	Sex	Age Class	Mass (g)	SVL (mm)	Tail (mm)
MAL_DR2007_01	-	-	May 21, 2007	Male	Adult	-	-	-
MAL_DR2010_01	Mahler 1838	MCZ R-188778	March 22, 2010	Female	Adult	-	133	176
DLM_DR2010b_02	Mahler 1864	MCZ R-188774	April 1, 2010[1]	Male	Adult	41.4[1]	124	151
DLM_DR2010b_01	Mahler 1861	MCZ R-188777	April 1, 2010[2]	Female	Adult	41.5[2]	131	165
MAL_DR2010_02	-	-	April, 2010	Male	Adult	-	-	-
MAL_DR2010_03	-	-	May 1, 2010	Male	Adult	-	-	-
MAL_DR2010_04	-	-	May 1, 2010	Male	Adult	-	-	-
MAL_DR2010_05	-	-	May 4, 2010	Female	Adult	-	-	-
MAL_DR2010_06	GLOR 07567	MCZ R-188776	July 7, 2010	Male	Adult	-	125	168
MAL_DR2010_07	GLOR 07566	MCZ R-188779/ MNHNSD 23.2979	July 7, 2010	Female	Adult	-	125	162
MAL_DR2011_01	GLOR 07803	MCZ R-188775	January 22, 2011	Male	Adult	-	132	178
DLM_DR2011_11	-	-	May 21, 2011	Male	Adult	41.0	135	176
MAL_DR2011_02	-	-	May 21, 2011	Female	Juvenile	-	-	-
DLM_DR2011_13	-	-	June 9, 2011	-	Juvenile	-	-	-
DLM_DR2011_12	-	-	June 10-11, 2011	Male	Juvenile	4.3	60	74
-	Mahler 1862	MCZ R-188781	October 21, 2010[3]	Female	Juvenile	5.7[3]	63	70
-	Mahler 1863	MCZ R-188780	December 6, 2010[4]	Male	Juvenile	9.1[4]	72	78

[1.] Kept in captivity for study. On May 11, 2010, mass = 33.5 g. On October 21, 2010, mass = 36.8 g, SVL = 122 mm, Tail = 150.25 mm. Preserved July 23, 2011.

[2.] Kept in captivity for study. Laid 6 eggs in late 2010 (see text). On April 12, 2010, mass = 40.0 g. On May 11, 2010, mass = 40.4 g. On October 21, 2010, mass = 40.8 g, SVL = 125.94 mm, Tail = 163 mm. Preserved July 2, 2011.

[3.] Date refers to hatching date. Egg laid in September, 2010 by MCZ R-188777. Upon hatching on Oct. 21, 2010, mass = 2.0 g, SVL = 41 mm, Tail = 50 mm. Preserved as juvenile on July 23, 2011.

[4.] Date refers to hatching date. Egg laid in September or October, 2010 by MCZ R-188777. Upon hatching on Dec. 6, 2010, mass = 2.1 g, SVL = 42.7 mm, Tail = 50.48 mm. Preserved as juvenile on July 23, 2011.

Table S2. Meristic traits for the type series of *Anolis landestoyi* sp. nov. See (Williams et al. 1995) for detailed descriptions of all characters except lamella number. For that trait, we instead report the total count of enlarged subdigital scales (or aberrantly, adjacent pairs of scales) under the digit of hindtoe IV (phalanges ii-iv). For paired traits, left and right scores are separated by a comma. A dash indicates "not applicable."

	MCZ R-188774	**MCZ R-188775**	**MCZ R-188776**	**MCZ R-188777**	**MCZ R-188778**	**MCZ R-188779**	**MCZ R-188780**	**MCZ R-188781**
Sex	M	M	M	F	F	F	M (J)	F (J)
Head scales	rugose	rugose	rugose	rugose	rugose	rugose	unicarinate	unicarinate
Scales b/t 2nd canthals	7	7	7	7	8	8	9	8
Postrostrals	6	6	5	5[1]	5	5	5	5
Nasal	circumnasal	circumnasal	circumnasal	circumnasal	circumnasal	circumnasal	circumnasal	circumnasal
Scales b/t nasal and rostral	1,1	1,1	1,1	1,1	1,1	1,1	1,1	1,1
Scales b/t supraorbital semicircles	2	3	3	3	3	3	2	2
Elongate superciliaries	3,2	2,2	2,2	3,2	3,3	2,2	2,3	2,1
Superciliary series	small scales	small scales	small scales	small scales	small scales	small scales	small scales	small scales
Loreal rows	5,5	7,6	7,6	6,7	6,6	6,7	7,7	6,5
Interparietal relative to ear	equal to	equal to	equal to	equal to	equal to or slightly larger	equal to	equal to	equal to
Scales b/t interparietal and semicircles	3,4	4,4	3,3	4,4	5,5	5,5	4,4	5,5
Scale rows b/t suboculars and supralabials	0,0	0,0	0,0	0,0	0,0	0,0	0,0	0,0
Supralabials to below center of eye	9,10	8,9	10,9	9,9	10,10	9,8	9,10	9,9
Postmentals	6	6	8	8	8	6	8	8
Sublabials	present	present	present	present	present	present	present	present
Sublabials in contact with infralabials	4,5	4,4	5,4	4,4	4,4	5,4	5,4	4,4

[1.] Note that rostral in this specimen is deformed and not fully present on right side.

Table S2 (Continued)

	MCZ R-188774	MCZ R-188775	MCZ R-188776	MCZ R-188777	MCZ R-188778	MCZ R-188779	MCZ R-188780	MCZ R-188781
Dorsals	flat, smooth to unicarinate	flat, smooth to unicarinate	flat, smooth to unicarinate	flat, smooth to unicarinate	flat, smooth to unicarinate	flat, smooth to unicarinate	flat, smooth to unicarinate	flat, smooth to unicarinate
Middorsal crests	high crest	high crest	high crest	high crest	high crest	high crest	high crest	high crest
Flank scales	partial contact	partial contact	partial contact	partial contact	partial contact	partial contact	partial contact	partial contact
Size of ventrals relative to dorsals	smaller	smaller	smaller	smaller	smaller	smaller	smaller	smaller
Smooth or keeled ventrals	strongly keeled to weakly keeled	strongly keeled to weakly keeled	strongly keeled to weakly keeled	strongly keeled to weakly keeled	strongly keeled to weakly keeled	strongly keeled to weakly keeled	strongly keeled to weakly keeled	strongly keeled to weakly keeled
Ventrals	subimbricate	subimbricate	subimbricate	subimbricate	subimbricate	subimbricate	subimbricate	subimbricate
Toepads	pad overlapping first phalanx	pad overlapping first phalanx	pad overlapping first phalanx	pad overlapping first phalanx	pad overlapping first phalanx	pad overlapping first phalanx	pad overlapping first phalanx	pad overlapping first phalanx
Lamella number	43,45	41,43	43,46	41,42	45,47	42,44	45,43	45,44
Supradigitals	multicarinate	multicarinate	multicarinate	multicarinate	multicarinate	multicarinate	multicarinate	multicarinate
Tail shape	strongly compressed	strongly compressed	strongly compressed	strongly compressed	strongly compressed	strongly compressed	strongly compressed	strongly compressed
Tail crest	serrated to distinct crest	serrated to distinct crest	serrated to distinct crest	serrated to distinct crest	serrated to distinct crest	serrated to distinct crest	serrated to distinct crest	serrated to distinct crest
Enlarged postanals	present	present	present	absent	absent	absent	present	absent
Male dewlap	large	large	large	-	-	-	large	-
Female dewlap	-	-	-	large	large	large	-	large

Table S3. Species level meristic variation for *Anolis landestoyi* sp. nov. compared to several species of Greater Antillean *Anolis*. Values for *A. landestoyi* and *A. ricordii* were scored directly from specimens; values for other species were obtained from Williams et al. (1995), which also contains detailed character descriptions. Ranges indicate minimum and maximum value observed for each species sample.

	landestoyi	***ricordii***[1]	***baleatus***	***barahonae***	***eugenegrahami***	***christophei***	***darlingtoni***	***insolitus***	***barbatus***	***porcus***
Sample (n)	8	7	20	20	10	20	4	3	6	2
Head scales	rugose to unicarinate	rugose	rugose to unicarinate	smooth to unicarinate	rugose to multicarinate	smooth to unicarinate	smooth to rugose	smooth	rugose	rugose
Scales b/t 2nd canthals	7-9	4-9	2-7	4-8	12-15	6-12	3-5	3-4	6-7	5-11
Postrostrals	5-6	6-7	4-8	5-8	4-11	4-10	6	4-9	6-7	5-7
Nasal	circumnasal	circumnasal	circumnasal to divided anterior nasal	circumnasal to anterior nasal	circumnasal to divided anterior nasal	circumnasal to inferior nasal	circumnasal	circumnasal	circumnasal	circumnasal
Scales b/t nasal and rostral	1	1-2	0-2	0-3	0-2	0-2	1	1	3-4	3-5
Scales b/t supraorbital semicircles	2-3	2-3	1-4	2-3	2-4	1-2	0-1	1	2-4	5
Elongate superciliaries	1-3	2-4	1-4	1-4	2-4	1-3	0-3	0	1	1
Superciliary series	small scales	granules to small scales	granules to small scales	granules to small scales	granules to small scales	granules to small scales	granules to small scales	granules to small scales	granules to small scales	small scales
Loreal rows	5-7	4-7	5-10	5-8	5-8	4-8	2-4	2-4	3-6	5
Interparietal relative to ear	equal to or larger	much smaller to smaller	much smaller to larger	much smaller to smaller	much smaller to smaller	smaller to equal to	larger to much larger	larger to much larger	smaller to equal to	smaller
Scales b/t interparietal and semicircles	3-5	3-5	3-7	3-5	6-10	3-7	0-1	0-2	3-5	4-6
Scale rows b/t suboculars and supralabials	0	0-1	0-1	0-2	0-1	0-1	0	0	0-1	0-1
Supralabials to below center of eye	8-10	8-11	8-11	8-11	6-9	6-8	6-8	6-7	9-11	11-12
Postmentals	6-8	6-8	4-8	4-12	5-12	6-12	4-5	5-10	4-8	5-7
Sublabials	present	present	present	present	present	present	present	present	absent to present	absent to present
Sublabials in contact with infralabials	4-5	1-4	2-4	1-5	0	1-2	3-4	2-4	1-8	0-10

Table S3 (Continued)

	landestoyi	***ricordii***[1]	***baleatus***	***barahonae***	***eugenegrahami***	***christophei***	***darlingtoni***	***insolitus***	***barbatus***	***porcus***
Dorsals	flat, smooth to unicarinate	unicarinate to conical crest scales	unicarinate to triangular or conical crest scales	swollen to triangular or conical crest scales	flat, smooth to unicarinate	flat, smooth to unicarinate	flat, smooth	flat, smooth	triangular or conical crest scales	flat, smooth
Middorsal crests	high crest	low crest to high crest	none to high crests	none to high crests	none	none	none	none	low crest	none
Flank scales	partial contact	partial contact	partial contact	partial contact	partial contact	partial contact	partial contact	partial contact	more or less widely separated[2]	more or less widely separated
Size of ventrals relative to dorsals	smaller	equal to smaller	larger to smaller	larger to smaller	larger to smaller	larger	smaller	larger	larger to much smaller	larger to smaller
Smooth or keeled ventrals	weakly to strongly keeled	smooth to weakly keeled	smooth to strongly keeled	smooth to strongly keeled	smooth to strongly keeled	smooth	smooth	smooth	smooth	smooth
Ventrals	subimbricate	subimbricate	juxtaposed to imbricate	separated to imbricate	separated to subimbricate	separated to imbricate	juxtaposed to imbricate	separated to subimbricate	juxtaposed	separated to juxtaposed
Toepads	pad overlapping first phalanx	pad overlapping first phalanx	pad overlapping first phalanx	pad overlapping first phalanx	pad overlapping first phalanx	pad overlapping first phalanx	pad overlapping first phalanx	pad overlapping first phalanx	pad overlapping first phalanx	pad overlapping first phalanx
Supradigitals	multicarinate	multicarinate	multicarinate	multicarinate	multicarinate	multicarinate	multicarinate	smooth to multicarinate	smooth	smooth
Tail shape	strongly compressed	strongly compressed	strongly compressed	weakly to strongly compressed	weakly to strongly compressed	round to weakly compressed	weakly to strongly compressed	round to weakly compressed	strongly compressed	strongly compressed
Tail crest	serrated to distinct crest	serrate to high crest	serrate to high crest	none to high crest	none to distinct crest	none to serrate	none	serrate	none to serrate	none to distinct crest
Enlarged postanals	present	present	present to absent	present to absent	present to absent	present to absent	present to absent	present to absent	present to absent	present to absent
Male dewlap	large	large	large	large	large to small	large	large	large	large	large
Female dewlap	large	large	large	large	intermediate to absent	small to absent	unknown	large	large	large

[1.] *Anolis ricordii* specimens examined: MCZ R-8619, MCZ R-65731, MCZ R-80945, MCZ R-80947, MCZ R-80953, MCZ R-130268, MCZ R-130274.

[2.] Our score differs from Williams et al. (1995), who marked this species as "juxtaposed to imbricate." We consider that to be an error based on reexamination of the original specimens.

Table S4. External measurements for all preserved specimens of *Anolis landestoyi* sp. nov. For paired traits, measurements were taken from the right side of the specimen (except lamella number, for which we present averages of left and right counts). Traits measured correspond to those presented in Mahler et al. (2010).

Specimen	SVL	Tail length	Head length	Head width	Head height	Lower jaw length	Quadrate to rostral scale	Jugal to rostral scale	Femur length	Tibia length	Metatarsal IV length
MCZ R-188780	72.00	78.00	21.12	12.69	10.84	22.11	20.34	16.37	16.00	12.76	8.11
MCZ R-188775	132.00	178.00	39.22	20.03	18.23	39.60	36.50	29.40	26.21	22.31	14.13
MCZ R-188776	124.74	168.00	35.99	18.31	16.80	36.95	34.02	27.75	27.46	21.39	13.61
MCZ R-188774	124.00	151.00	36.85	20.02	18.30	38.47	35.35	28.31	26.83	20.85	13.39
MCZ R-188781	62.87	70.00	19.10	10.91	9.47	19.65	18.04	14.94	13.00	10.63	7.12
MCZ R-188778	133.40	176.00	38.93	20.40	18.42	39.46	36.38	29.49	27.85	21.55	13.86
MCZ R-188777	131.31	165.00	37.25	18.78	17.33	38.30	35.44	28.67	25.71	20.22	13.04
MCZ R-188779	124.78	162.00	36.27	18.04	17.90	36.32	33.47	27.19	26.16	21.04	13.99

Specimen	Toe IV length	Lamella width, toe IV	Lamella number, toe IV	Humerus length	Radius length	Metacarpal IV length	Foretoe IV length	Lamella width, foretoe IV	Lamella number, foretoe IV
MCZ R-188780	11.45	1.48	44.00	13.59	10.65	3.05	6.58	1.27	24.50
MCZ R-188775	20.44	2.60	42.00	24.88	20.50	6.14	12.59	2.38	27.00
MCZ R-188776	18.65	2.27	44.50	23.53	18.27	5.48	12.20	2.04	27.00
MCZ R-188774	20.05	2.51	44.00	23.97	19.18	5.49	11.58	2.05	28.00
MCZ R-188781	10.60	1.40	44.50	11.70	9.07	3.04	6.58	1.18	26.50
MCZ R-188778	20.15	2.68	46.00	24.85	18.72	5.79	12.49	2.46	27.50
MCZ R-188777	19.46	2.41	41.50	22.81	18.55	5.29	11.90	2.30	25.00
MCZ R-188779	18.80	2.10	43.00	23.81	18.36	5.40	11.23	1.97	25.00

Specimen	Pelvis height	Pelvis width
MCZ R-188780	7.63	6.60
MCZ R-188775	14.26	10.03
MCZ R-188776	13.34	10.59
MCZ R-188774	14.96	10.12
MCZ R-188781	6.68	6.12
MCZ R-188778	16.73	10.53
MCZ R-188777	16.72	11.05
MCZ R-188779	15.29	10.71

[1.] We counted lamellae as the total number of enlarged subdigital scales (or aberrantly, adjacent pairs of scales) under the digit of hindtoe IV (phalanges ii-iv).

Table S5. Euclidean distances separating *Anolis landestoyi* sp. nov. from other Greater Antillean anole species in a morphospace defined by the first four axes of a phylogenetic PCA on body size and several ecomorphological shape traits. "Ecomorph" refers to the habitat specialist class to which each species has been assigned, with "unique" being unassigned to one of the seven ecomorph categories (Losos 2009).

Species	Euclidean distance	Ecomorph
guamuhaya	0.31	Twig-Giant
porcus	0.32	Twig-Giant
chamaeleonides	0.39	Twig-Giant
barahonae	0.50	Crown-Giant
baleatus	0.51	Crown-Giant
ricordii	0.53	Crown-Giant
valencienni	0.57	Twig
equestris	0.61	Crown-Giant
allisoni	0.65	Trunk-Crown
vermiculatus	0.69	Unique
cuvieri	0.73	Crown-Giant
smallwoodi	0.75	Crown-Giant
coelestinus	0.77	Trunk-Crown
chlorocyanus	0.79	Trunk-Crown
porcatus	0.82	Trunk-Crown
aliniger	0.87	Trunk-Crown
singularis	0.88	Trunk-Crown
cristatellus	0.91	Trunk-Ground
grahami	0.94	Trunk-Crown
cybotes	0.99	Trunk-Ground
sagrei	1.00	Trunk-Ground
evermanni	1.00	Trunk-Crown
reconditus	1.01	Unique
armouri	1.01	Trunk-Ground
fowleri	1.02	Unique
jubar	1.04	Trunk-Ground
rubribarbus	1.04	Trunk-Ground
cooki	1.05	Trunk-Ground
imias	1.05	Trunk-Ground
bartschi	1.06	Unique
strahmi	1.07	Trunk-Ground
lineatopus	1.07	Trunk-Ground
mestrei	1.07	Trunk-Ground
marcanoi	1.08	Trunk-Ground
stratulus	1.09	Trunk-Crown
quadriocellifer	1.09	Trunk-Ground
insolitus	1.10	Twig
shrevei	1.11	Trunk-Ground
whitemani	1.11	Trunk-Ground
longitibialis	1.11	Trunk-Ground
altitudinalis	1.11	Trunk-Crown
angusticeps	1.12	Twig
gundlachi	1.12	Trunk-Ground
distichus	1.12	Trunk
lucius	1.13	Unique
brevirostris	1.13	Trunk
guafe	1.13	Trunk-Ground
loysiana	1.14	Trunk
opalinus	1.18	Trunk-Crown
centralis	1.19	Unique
eugenegrahami	1.26	Unique
christophei	1.26	Unique
dolichocephalus	1.27	Grass-Bush
argenteolus	1.29	Unique
pulchellus	1.29	Grass-Bush
placidus	1.33	Twig
krugi	1.33	Grass-Bush
hendersoni	1.33	Grass-Bush
bahorucoensis	1.34	Grass-Bush
guazuma	1.36	Twig
ophiolepis	1.36	Grass-Bush
pumilus	1.41	Unique
vanidicus	1.41	Grass-Bush
olssoni	1.46	Grass-Bush
barbouri	1.46	Unique
occultus	1.47	Twig
alutaceus	1.52	Grass-Bush
semilineatus	1.53	Grass-Bush
cyanopleurus	1.55	Grass-Bush
sheplani	1.58	Twig
etheridgei	1.60	Unique

Table S6. Results of a linear discriminant analysis on ecomorph class (seven categories) for Greater Antillean anole species previously assigned to an ecomorph (56 species included in this study) as well as those hypothesized in this paper to represent a new ecomorph class (four species); CG = crown-giant, GB = grass-bush, TC = trunk-crown, TG = trunk-ground, TR = trunk, TW = twig, TwG = twig-giant. "Ecomorph Prior" refers to the *a priori* ecomorph class assignment, and "Ecomorph Posterior" refers to the LDA classification, assigned by majority-rule posterior probability in a leave-one-out cross-validation procedure. Posterior probabilities for each ecomorph class (pp) are presented.

Species	Ecomorph Prior	Ecomorph Posterior	Trunk-Ground (pp)	Trunk-Crown (pp)	Crown-Giant (pp)	Twig (pp)	Grass-Bush (pp)	Trunk (pp)	Twig-Giant (pp)
landestoyi	TwG	TwG	0.00	0.00	0.03	0.00	0.00	0.00	0.97
chamaeleonides	TwG	TwG	0.00	0.00	0.00	0.00	0.00	0.00	1.00
guamuhaya	TwG	TwG	0.00	0.00	0.00	0.00	0.00	0.00	1.00
porcus	TwG	TwG	0.00	0.00	0.00	0.00	0.00	0.00	1.00
baleatus	CG	CG	0.00	0.00	1.00	0.00	0.00	0.00	0.00
barahonae	CG	CG	0.00	0.00	1.00	0.00	0.00	0.00	0.00
cuvieri	CG	CG	0.00	0.00	1.00	0.00	0.00	0.00	0.00
equestris	CG	CG	0.00	0.00	1.00	0.00	0.00	0.00	0.00
ricordii	CG	CG	0.00	0.00	1.00	0.00	0.00	0.00	0.00
smallwoodi	CG	CG	0.00	0.00	1.00	0.00	0.00	0.00	0.00
alutaceus	GB	GB	0.00	0.00	0.00	0.00	1.00	0.00	0.00
bahorucoensis	GB	GB	0.00	0.00	0.00	0.00	1.00	0.00	0.00
cyanopleurus	GB	GB	0.00	0.00	0.00	0.00	1.00	0.00	0.00
dolichocephalus	GB	GB	0.00	0.00	0.00	0.00	1.00	0.00	0.00
hendersoni	GB	GB	0.00	0.00	0.00	0.00	1.00	0.00	0.00
krugi	GB	GB	0.00	0.00	0.00	0.00	1.00	0.00	0.00
olssoni	GB	GB	0.00	0.00	0.00	0.00	1.00	0.00	0.00
ophiolepis	GB	GB	0.00	0.00	0.00	0.00	1.00	0.00	0.00
pulchellus	GB	GB	0.00	0.00	0.00	0.00	1.00	0.00	0.00
semilineatus	GB	GB	0.00	0.00	0.00	0.00	1.00	0.00	0.00
vanidicus	GB	GB	0.00	0.00	0.00	0.00	1.00	0.00	0.00
aliniger	TC	TC	0.00	1.00	0.00	0.00	0.00	0.00	0.00
allisoni	TC	TC	0.00	1.00	0.00	0.00	0.00	0.00	0.00
altitudinalis	TC	TW	0.00	0.38	0.00	0.62	0.00	0.00	0.00
chlorocyanus	TC	TC	0.00	1.00	0.00	0.00	0.00	0.00	0.00
coelestinus	TC	TC	0.00	1.00	0.00	0.00	0.00	0.00	0.00
evermanni	TC	TC	0.00	0.99	0.00	0.00	0.00	0.01	0.00
grahami	TC	TC	0.01	0.99	0.00	0.00	0.00	0.00	0.00
opalinus	TC	TR	0.05	0.19	0.00	0.00	0.00	0.76	0.00
porcatus	TC	TC	0.00	1.00	0.00	0.00	0.00	0.00	0.00
singularis	TC	TC	0.00	1.00	0.00	0.00	0.00	0.00	0.00
stratulus	TC	TR	0.01	0.35	0.00	0.00	0.00	0.64	0.00
armouri	TG	TG	1.00	0.00	0.00	0.00	0.00	0.00	0.00
cooki	TG	TG	0.93	0.07	0.00	0.00	0.00	0.00	0.00
cristatellus	TG	TG	0.96	0.02	0.00	0.00	0.00	0.02	0.00
cybotes	TG	TG	1.00	0.00	0.00	0.00	0.00	0.00	0.00
guafe	TG	TG	0.53	0.00	0.00	0.00	0.00	0.47	0.00
gundlachi	TG	TG	1.00	0.00	0.00	0.00	0.00	0.00	0.00
imias	TG	TG	1.00	0.00	0.00	0.00	0.00	0.00	0.00
jubar	TG	TG	0.80	0.00	0.00	0.00	0.00	0.20	0.00
lineatopus	TG	TG	1.00	0.00	0.00	0.00	0.00	0.00	0.00
longitibialis	TG	TG	1.00	0.00	0.00	0.00	0.00	0.00	0.00
marcanoi	TG	TG	0.99	0.00	0.00	0.00	0.00	0.00	0.00
mestrei	TG	TG	0.96	0.00	0.00	0.00	0.00	0.04	0.00
quadriocellifer	TG	TG	0.95	0.00	0.00	0.00	0.00	0.05	0.00
rubribarbus	TG	TG	1.00	0.00	0.00	0.00	0.00	0.00	0.00

Table S6 (Continued).

Species	Ecomorph Prior	Ecomorph Posterior	Trunk-Ground (pp)	Trunk-Crown (pp)	Crown-Giant (pp)	Twig (pp)	Grass-Bush (pp)	Trunk (pp)	Twig-Giant (pp)
sagrei	TG	TG	0.93	0.07	0.00	0.00	0.00	0.00	0.00
shrevei	TG	TG	1.00	0.00	0.00	0.00	0.00	0.00	0.00
strahmi	TG	TG	1.00	0.00	0.00	0.00	0.00	0.00	0.00
whitemani	TG	TG	1.00	0.00	0.00	0.00	0.00	0.00	0.00
brevirostris	TR	TR	0.07	0.00	0.00	0.00	0.00	0.93	0.00
distichus	TR	TR	0.18	0.00	0.00	0.00	0.00	0.82	0.00
loysiana	TR	TR	0.09	0.39	0.00	0.01	0.00	0.51	0.00
angusticeps	TW	TW	0.00	0.28	0.00	0.72	0.00	0.00	0.00
guazuma	TW	TW	0.00	0.00	0.00	1.00	0.00	0.00	0.00
insolitus	TW	TW	0.00	0.00	0.00	1.00	0.00	0.00	0.00
occultus	TW	TW	0.00	0.00	0.00	1.00	0.00	0.00	0.00
placidus	TW	TW	0.00	0.00	0.00	1.00	0.00	0.00	0.00
sheplani	TW	TW	0.00	0.00	0.00	1.00	0.00	0.00	0.00
valencienni	TW	TC	0.00	0.97	0.00	0.03	0.00	0.00	0.00

Table S7. Individuals from the *ricordii* clade of *Anolis* that were collected for this study, with associated catalog numbers. Field tag numbers and species names correspond to tip labels in the figures depicting the *ricordii*-clade phylogenetic results. A dash indicates missing information.

Species	Sex	Age Class	Field Tag
A. baleatus	-	-	GLOR 1089
A. baleatus	-	-	GLOR 1090
A. baleatus	-	-	GLOR 1091
A. baleatus	-	-	GLOR 1092
A. baleatus	-	-	GLOR 1093
A. baleatus	-	-	GLOR 1112
A. baleatus	-	-	GLOR 1124
A. baleatus	-	-	GLOR 1125
A. baleatus	-	-	GLOR 1126
A. baleatus	-	-	GLOR 1136
A. baleatus	-	Juvenile	GLOR 1141
A. baleatus	-	Juvenile	GLOR 1142
A. baleatus	-	Adult	GLOR 1143
A. baleatus	-	Adult	GLOR 1144
A. baleatus	-	Adult	GLOR 1145
A. baleatus	-	Adult	GLOR 1146
A. baleatus	-	Adult	GLOR 1164
A. baleatus	-	Adult	GLOR 1165
A. baleatus	-	Juvenile	GLOR 1166
A. baleatus	-	Juvenile	GLOR 1167
A. baleatus	-	Juvenile	GLOR 1168
A. baleatus	-	Juvenile	GLOR 1169
A. baleatus	-	Juvenile	GLOR 1170
A. baleatus	-	-	GLOR 1201
A. baleatus	-	-	GLOR 1202
A. baleatus	-	-	GLOR 1255
A. baleatus	-	-	GLOR 1278
A. baleatus	-	-	GLOR 1292
A. baleatus	-	-	GLOR 1298
A. baleatus	-	-	GLOR 1299
A. baleatus	-	-	GLOR 1300
A. baleatus	-	-	GLOR 1301
A. baleatus	-	-	GLOR 1308
A. baleatus	-	-	GLOR 1328
A. baleatus	-	-	GLOR 1329
A. baleatus	-	-	GLOR 1330
A. baleatus	-	-	GLOR 1331
A. baleatus	Female	Juvenile	GLOR 1501
A. baleatus	Male	Juvenile	GLOR 3765
A. baleatus	Female	Juvenile	GLOR 5598
A. baleatus	Female	Juvenile	GLOR 5599
A. baleatus	Male	Adult	GLOR 6791
A. barahonae	-	-	GLOR 1425
A. barahonae	-	-	GLOR 1427
A. barahonae	-	-	GLOR 1429
A. barahonae	-	-	GLOR 1430
A. barahonae	-	-	GLOR 1431
A. barahonae	-	-	GLOR 1432
A. barahonae	-	-	GLOR 1433
A. ricordii	-	-	GLOR 1336
A. ricordii	-	-	GLOR 1343
A. ricordii	-	-	GLOR 1344
A. ricordii	-	-	GLOR 1345
A. ricordii	-	-	GLOR 1346
A. ricordii	Male	Adult	GLOR 7788
A. ricordii	Male	Subadult	GLOR 7789
A. ricordii	Male	Adult	GLOR 7790
A. ricordii	Male	Adult	GLOR 7791
A. ricordii	Female	Subadult	GLOR 7792
A. ricordii	Female	Adult	GLOR 7793
A. ricordii	Female	Juvenile	GLOR 7794
A. ricordii	Male	Adult	GLOR 7799

Table S8. Outline of analyses conducted to assess the phylogenetic affinities of *Anolis landestoyi* sp. nov. We conducted analyses at both broad and narrow phylogenetic scales, using Bayesian methods on both nuclear and mitochondrial DNA.

	Phylogenetic position of *A. landstoyi* within *Anolis*	**Phylogenetic position of *A. landestoyi* within Hispaniolan giant anoles (*ricordii* clade)**				
Data used to infer phylogenetic relationships	Nuclear DNA (5 nDNA genes; concatenated; partitioned)	Gene-trees (9 nDNA, 1 mtDNA)		Nuclear DNA (9 nDNA genes; concatenated; partitioned)	Nuclear DNA + mitochondrial DNA (9 nDNA genes, 1 mtDNA gene; concatenated; partitioned)	DNA for individual genes (separate analyses for each of 9 nDNA and 1mtDNA genes)
Program used for analysis	BEAST (MrBayes to generate starting tree)	*BEAST	BUCKy (MrBayes to generate individual gene-trees)	MrBayes	MrBayes	MrBayes
Species sample (ingroup only)	95 *Anolis* spp. (1 individual / sp.)	4 *Anolis* spp. 65 individuals (3-42 individuals / sp.)	4 *Anolis* spp. 65 individuals[1] (1 individual / sp.)	4 *Anolis* spp. 65 individuals (3-42 individuals / sp.)	4 *Anolis* spp. 65 individuals (3-42 individuals / sp.)	4 *Anolis* spp. 65 individuals (3-42 individuals / sp.)
Loci included in analyses	BDNF, GJA, NT3, RAG1, R35	RAG1, ROD, R35, BDNF, NT3, B108, B120, B127, GJA1, ND2	RAG1, ROD, R35, BDNF, NT3, B108, B120, B127, GJA1, ND2	RAG1, ROD, R35, BDNF, NT3, B108, B120, B127, GJA1	RAG1, ROD, R35, BDNF, NT3, B108, B120, B127, GJA1, ND2	RAG1, ROD, R35, BDNF, NT3, B108, B120, B127, GJA1, ND2

[1.] BUCKy randomly selected a single individual per species from our sample for each species-tree estimation. This process was repeated 100 times with replacement.

Table S9. Loci and primer sequences for the nucleotide sequence data used in our study.

Locus	Aligned Base Pairs	Primer Sequences	Source
ND2	1051	Metf.6, 5'-AAGCTTTCGGGCCCATACC-3' / Asnr.REG1, 5'-AGCGAATRGAAGCCCGCTGG-3'	Macey et al. (1997) (Metf.6); Glor et al. (2003) (Asnr.REG1)
RAG1	690	RAGMartfl.1, 5'-AGCTGCAGYCARTAYCAYAARATGTA-3' / RAGr.1, 5'-AACTCAGCTGCATTKCCAATRTCA-3'	Chiari et al. (2004)
ROD	834	Rod3, 5'-AGGTACATCCCAGAAGGCATGCAC-3' / Rod4, 5'-CAGGATTGTAGATGGCTGAGCT-3'	Glor et al. (2004)
R35	622	R35F, 5'-GACTGTGGAYGAYCTGATCAGTGTGGTGCC-3' / R35R, 5'-GCCAAAATGAGSGAGAARCGCTTCTGAGC-3'	Leaché (2009)
BDNF	771	BDNFf.2, 5'-GAAGAGTGATGACCATCCTTTTCC-3' / BDNFr.4, 5'-GAAYCACTGTACTGTATAAACTTC-3'	Noonan and Chippindale (2006)
NT3	510	NT3f, 5'-ATATTTCTGGCTTTTCTCTGTGGC-3' / NT3r, 5'-GCGTTTCATAAAAATATTGTTTGACCGG-3'	Noonan and Chippindale (2006)
B108	591	B108F, 5'-TGAGCAGCAACGTGAGAGAG-3' / B108R, 5'-GGCACTGGATGAACAGGTATC-3'	Alföldi et al. (2011)
B120	481	B120F, 5'-TGTCACCCTGATCAATTCCA-3' / B120R, 5'-CCTTGCCAGAATGACCAAAT-3'	Alföldi et al. (2011)
B127	347	B127F, 5'-AGTTGGGCCCATAGTGTGAG-3' / B127R, 5'-ATCACCTCTGATGACTCGGC-3'	Alföldi et al. (2011)
GJA1	1011	GJA1f.1, 5'-ATGGGTGACTGGAGYGC-3' / GJA1r.3, 5'-ATYTCCAGGTCATCAGGYCGAGG-3'	J. Schulte (pers. comm.)

Table S10. Models of molecular evolution selected for each partition for our estimates of *Anolis* phylogeny using concatenated data in BEAST, and for our species-tree (*BEAST, BUCKy) and concatenated (MrBayes) estimates of relationships within the *A. ricordii* species group.

Partition (Genus-wide)	**Model**	**Partition (*A. ricordii* group)**	**Model**
BDNF_1st	HKY+I	ND2	GTR+G
BDNF_2nd	HKY	B108	HKY
BDNF_3rd	HKY+G	B120	HKY+G
GJA_1st	GTR+I	B127	GTR+G
GJA_2nd	HKY	BDNF	HKY+G
GJA_3rd	GTR+G	GJA1	GTR+G
mtDNA_1st	GTR+G	NT3	HKY+G
mtDNA_2nd	HKY+G	R35	HKY+G
mtDNA_3rd	GTR+G	RAG1	GTR+G
mtDNA_tRNA	GTR+G	ROD (protein coding)	GTR+G
NT3_1st	GTR+I	ROD (intronic)	GTR+G
NT3_2nd	HKY+I		
NT3_3rd	GTR+G		
R35_1st	GTR+G		
R35_2nd	GTR+G		
R35_3rd	GTR+G		
RAG1_1st	GTR+G		
RAG1_2nd	HKY+I		
RAG1_3rd	HKY+G		

Table S11. Loadings, eigenvalues, and variance explained for the first four axes of a phylogenetic principal component analysis (pPCA) of 11 ecomorphological traits using the MCC chronogram from the posterior distribution of a Bayesian phylogenetic analysis of nucleotide data conducted in BEAST. Note, cumulative variances were calculated by summing unrounded variances rather than the rounded variances presented here.

Trait	**pPC 1**	**pPC 2**	**pPC 3**	**pPC 4**
Snout-to-vent length (SVL)	0.03	1.00	-0.01	0.00
Tail length	0.80	0.01	0.54	0.19
Femur length	0.90	-0.03	-0.19	-0.16
Tibia length	0.93	-0.03	-0.16	-0.12
Metatarsal IV length	0.97	-0.03	-0.04	-0.08
Toe IV length	0.92	-0.03	-0.07	-0.01
Humerus length	0.62	-0.03	-0.55	-0.19
Radius length	0.66	-0.03	-0.57	-0.27
Foretoe IV length	0.81	-0.03	-0.39	-0.15
Lamella number, toe IV	0.26	-0.01	-0.30	0.88
Lamella number, foretoe IV	0.02	0.00	-0.54	0.80
Eigenvalue	0.0063	0.0045	0.0017	0.0013
Variance Explained	0.43	0.30	0.11	0.09
Cumulative Variance Explained	0.43	0.73	0.85	0.94

Table S12. Species scores for the first four axes of a phylogenetic principal component analysis (pPCA) of 11 ecomorphological traits generated using the MCC chronogram from the posterior distribution of a Bayesian phylogenetic analysis of nuclear DNA data.

Species	pPC 1	pPC 2	pPC 3	pPC 4
aliniger	-0.22	-0.02	-0.13	0.18
allisoni	-0.19	0.33	0.10	0.22
altitudinalis	-0.68	-0.20	-0.16	0.31
alutaceus	0.24	-0.50	0.29	0.16
angusticeps	-0.65	-0.25	0.09	0.05
argenteolus	0.47	-0.10	-0.28	0.27
armouri	0.30	0.05	-0.12	-0.26
bahorucoensis	0.39	-0.24	0.20	0.04
baleatus	0.04	1.00	0.01	0.01
barahonae	0.03	1.02	0.01	-0.01
barbouri	0.23	-0.40	0.32	-0.49
bartschi	0.48	0.21	-0.21	0.13
brevirostris	0.15	-0.20	-0.38	-0.08
centralis	-0.21	-0.35	0.10	0.05
chamaeleonides	-0.65	0.99	-0.34	-0.11
chlorocyanus	-0.05	0.22	-0.01	0.31
christophei	0.41	-0.19	-0.31	-0.02
coelestinus	0.00	0.24	0.05	0.23
cooki	0.33	0.02	-0.01	-0.04
cristatellus	0.24	0.12	-0.20	-0.10
cuvieri	0.33	0.81	-0.02	-0.04
cyanopleurus	0.41	-0.43	0.38	0.04
cybotes	0.35	0.14	-0.11	-0.26
distichus	0.18	-0.15	-0.44	-0.15
dolichocephalus	0.25	-0.15	0.30	0.24
equestris	-0.04	1.06	-0.07	0.31
etheridgei	0.67	-0.42	-0.06	-0.12
eugenegrahami	0.61	0.05	-0.35	0.09
evermanni	0.24	0.10	-0.31	0.24
fowleri	0.38	0.23	0.23	-0.17
grahami	0.18	0.09	-0.20	0.18
guafe	0.18	-0.19	-0.28	-0.19
guamuhaya	-0.50	0.99	-0.28	0.05
guazuma	-1.20	-0.26	-0.06	0.10
gundlachi	0.45	0.11	-0.04	-0.42
hendersoni	0.34	-0.20	0.27	0.18

Species	pPC 1	pPC 2	pPC 3	pPC 4
imias	0.32	0.02	-0.23	-0.32
insolitus	-0.73	-0.24	-0.04	-0.17
jubar	0.13	-0.12	-0.25	-0.20
krugi	0.45	-0.18	0.16	0.11
landestoyi	-0.37	0.79	-0.17	-0.11
lineatopus	0.38	0.06	-0.05	-0.29
longitibialis	0.48	0.17	-0.08	-0.44
loysiana	-0.31	-0.35	-0.20	-0.04
lucius	0.48	0.12	-0.36	0.18
marcanoi	0.37	0.01	-0.08	-0.10
mestrei	0.24	-0.09	-0.22	-0.21
occultus	-1.26	-0.36	0.03	-0.01
olssoni	0.40	-0.26	0.46	0.08
opalinus	0.17	-0.23	-0.25	0.11
ophiolepis	0.05	-0.41	0.31	-0.11
placidus	-1.17	-0.25	0.05	-0.04
porcatus	-0.20	0.21	0.05	0.41
porcus	-0.60	0.99	-0.18	-0.04
pulchellus	0.24	-0.26	0.24	0.08
pumilus	-0.23	-0.58	0.04	0.09
quadriocellifer	0.15	-0.17	-0.18	-0.23
reconditus	0.54	0.41	-0.07	-0.25
ricordii	0.09	0.95	-0.01	0.01
rubribarbus	0.27	0.00	-0.22	-0.34
sagrei	0.21	0.00	0.01	-0.05
semilineatus	0.44	-0.36	0.41	0.09
sheplani	-1.42	-0.33	0.21	-0.03
shrevei	0.27	-0.09	-0.01	-0.26
singularis	-0.15	0.00	-0.11	0.21
smallwoodi	0.12	0.98	-0.11	0.42
strahmi	0.49	0.20	-0.21	-0.32
stratulus	0.02	-0.19	-0.28	0.12
valencienni	-0.54	0.28	-0.11	0.07
vanidicus	-0.09	-0.42	0.51	-0.08
vermiculatus	0.25	0.74	0.09	0.03
whitemani	0.38	0.03	0.01	-0.33

S4: SUPPLEMENTAL FIGURES

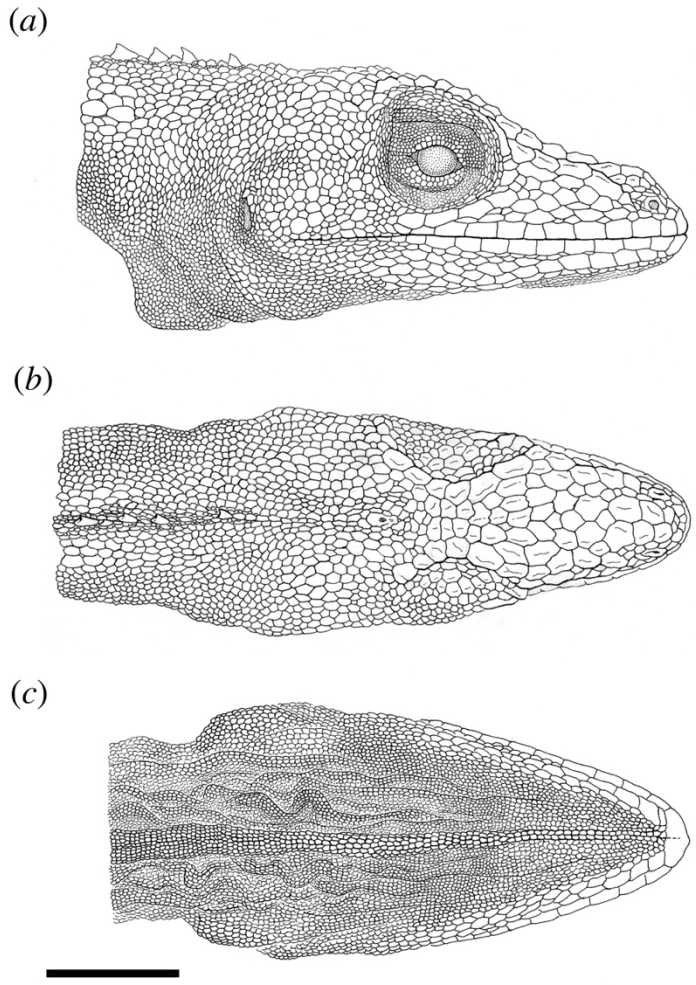

Figure S1. Right lateral (*a*), dorsal (*b*), and ventral (*c*) views of the head of the holotype of *Anolis landestoyi* sp. nov. (MCZ R-188774), illustrating scalation. Scale equals 10 mm. Illustrations by Laszlo Meszoly.

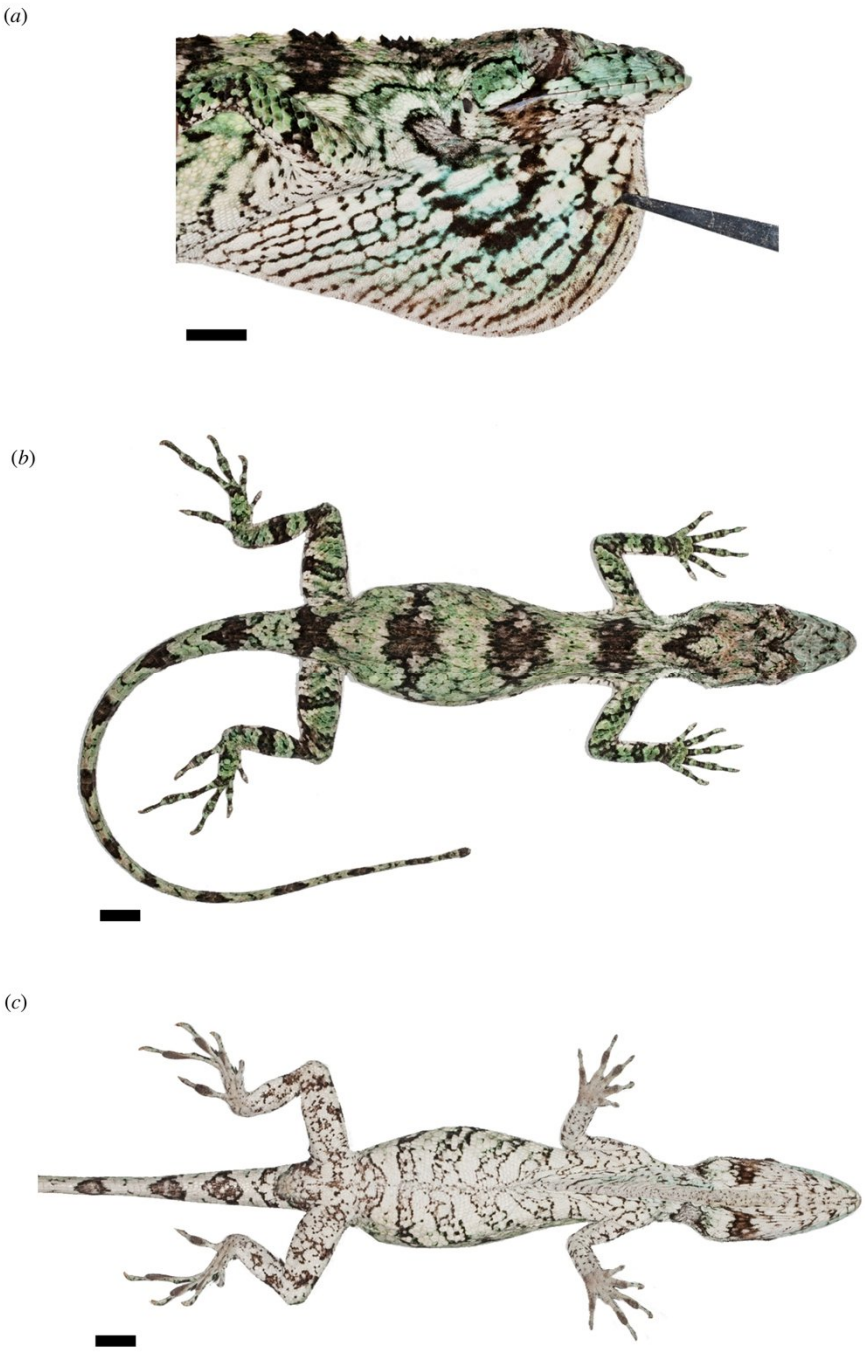

Figure S2. Female paratype (MCZ R-188777) of *Anolis landestoyi* sp. nov. in life. (*a*) Right lateral profile of head, with dewlap extended. (*b*) Dorsal view. (*c*) Ventral view. Scale equals 10 mm in all.

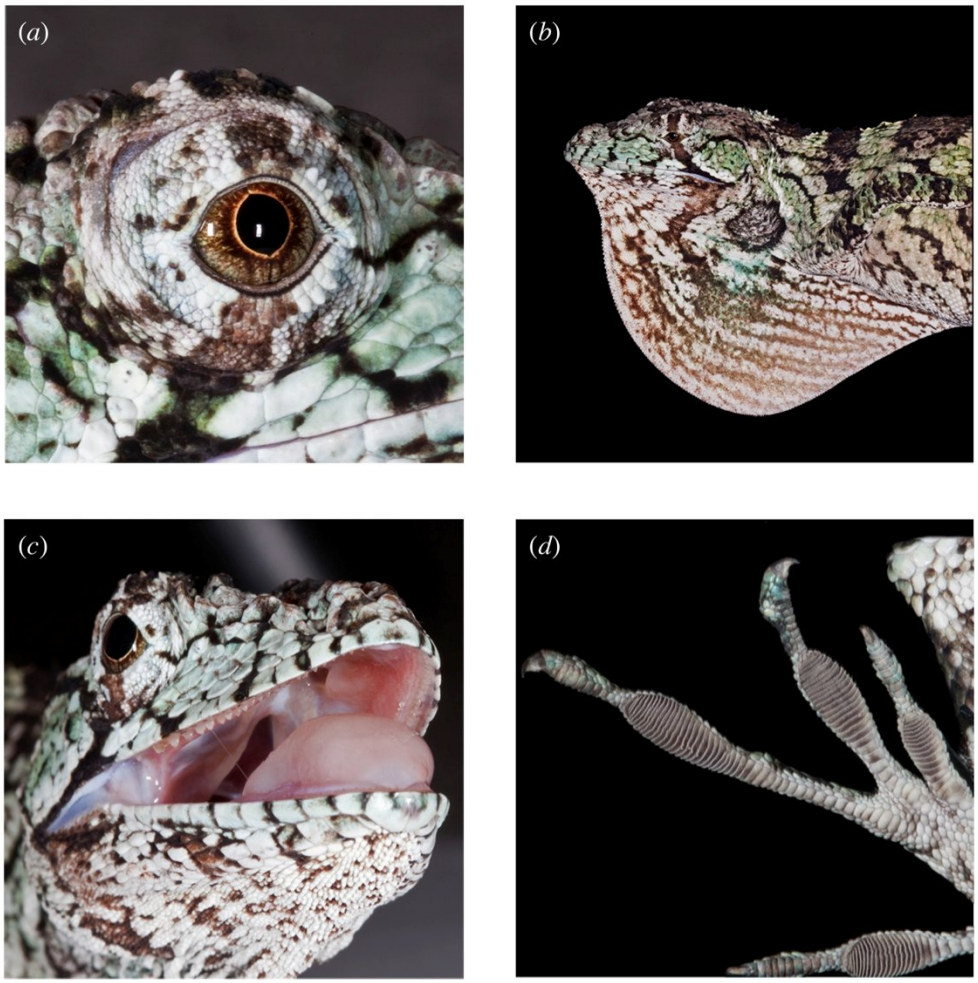

Figure S3. (*a*) Detail of the right eye of the holotype of *Anolis landestoyi* sp. nov. (MCZ R-188774) in life. (*b*) Right lateral profile of the holotype of *A. landestoyi* (MCZ R-188774) in life, with dewlap extended and darkened (contrast with figure 2a). (*c*) Tongue and lining of the mouth of the holotype of *A. landestoyi* (MCZ R-188774) in life. (*d*) Second, third, and fourth toes (right to left) of the right hindfoot of the holotype of *A. landestoyi* (MCZ R-188774) in life, illustrating subdigital lamellae and the shape of the claws.

Figure S4. A juvenile female paratype (MCZ R-188781) of *Anolis landestoyi* sp. nov., photographed within several hours of hatching on 21 October 2010. (*a*) Hatchling in left lateral view, posed next to its eggshell. Scale equals 10 mm. (*b*) Hatchling in hand, illustrating fully functional dewlap with adult patterning and coloration.

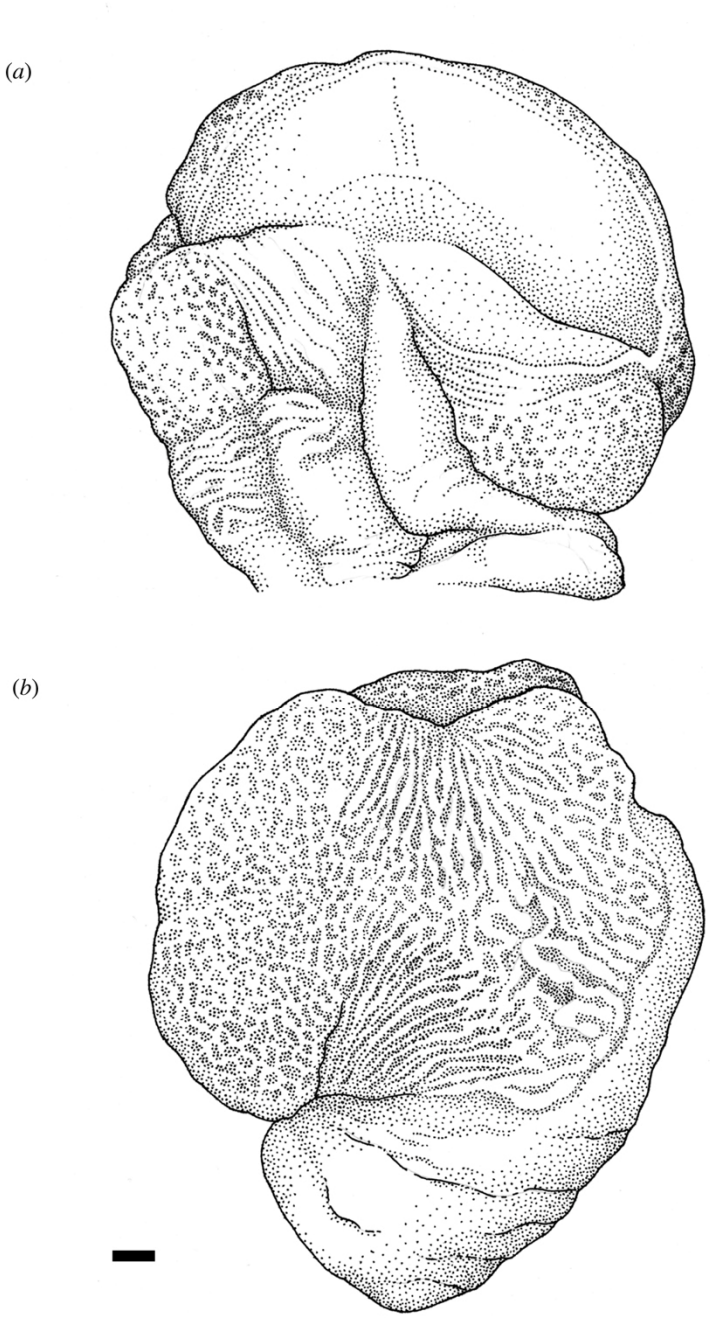

Figure S5. Sulcate (*a*) and asulcate (*b*) views of the left hemipenis of the holotype of *Anolis landestoyi* sp. nov. (MCZ R-188774). Scale equals 1 mm. Illustrations by Laszlo Meszoly.

Figure S6. (*a*-*b*) Representative dry forest habitat at the type locality of *Anolis landestoyi* sp. nov. in Reserva Biológica Loma Charco Azul (Independencia Province, Dominican Republic). Both photographs were taken in June, 2011 during the wet season. (*c*-*d*) Habitat destruction within the borders of Reserva Biológica Loma Charco Azul. Photograph (*c*) taken in July, 2013, courtesy Miguel Landestoy. Photograph (*d*) taken in July, 2013, courtesy Ernst Rupp, Grupo Jaragua.

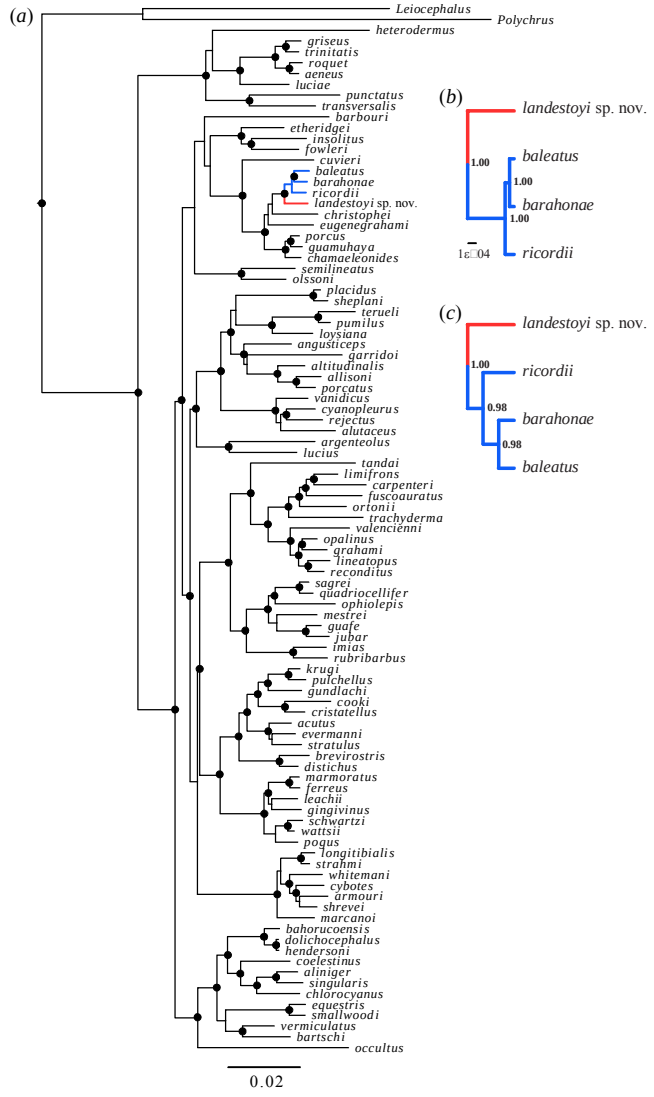

Figure S7. (*a*) Maximum clade credibility (MCC) topology from the posterior distribution of a MrBayes analysis of *Anolis* phylogeny (including two outgroups: *Leiocephalus* and *Polychrus*), based on five nuclear loci. Nodes with posterior probabilities of 0.95 or higher are indicated by black dots. (*b*-*c*) Phylogenetic relationships of the four species of Hispaniolan giant anoles, including *Anolis landestoyi* sp. nov., inferred using species-tree analyses of 65 individuals for nine nuclear genes and one mitochondrial gene. (*b*) MCC species-tree from a *BEAST concordance analysis. Node labels denote posterior probabilities (all nodes in this phylogeny have posterior probabilities of 1.0). (*c*) Species-tree inferred using BUCKy concordance analyses. Topology depicted is a 98% consensus tree of the concordance trees from 100 iterations of BUCKy. Node labels denote the proportion of concordance trees for which each node was recovered. In all panels, branches corresponding to *A. landestoyi* are colored red, while those corresponding to other Hispaniolan giant anole species are colored blue. For (*a*-*b*), branch lengths and scale bars are in proportion to nucleotide substitutions. For (*c*), branch lengths are arbitrary.

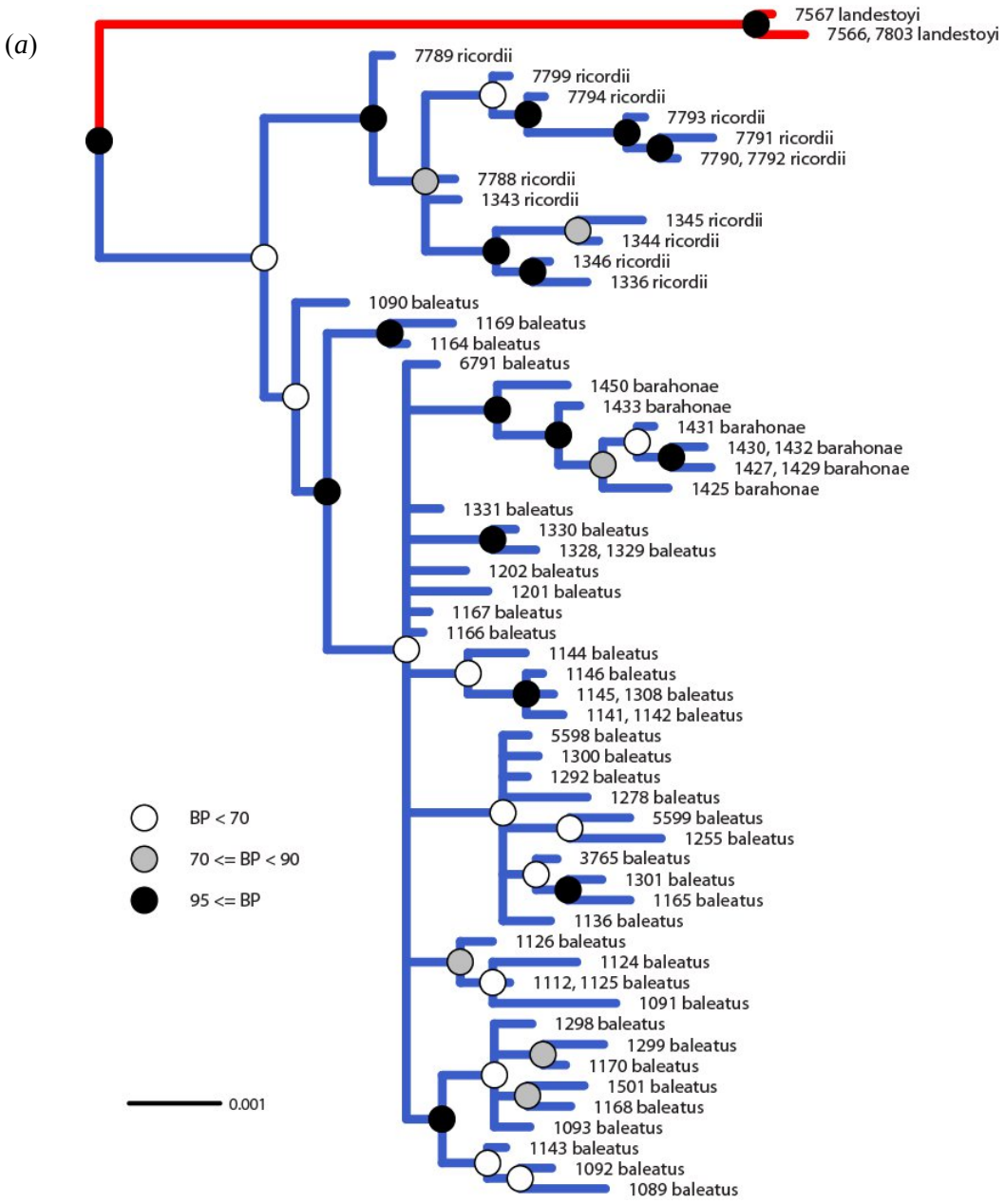

Figure S8. Phylogenetic relationships of the Hispaniolan giant anoles, including *Anolis landestoyi* sp. nov., inferred by Bayesian analysis of concatenated and individual loci. (*a*) Majority-rule consensus species-tree inferred from a MrBayes analysis of nine concatenated nuclear genes. (*b*) Majority-rule consensus species-tree inferred from a MrBayes analysis of the mitochondrial gene ND2. In both panels, branches corresponding to *A. landestoyi* are colored red, while those corresponding to other Hispaniolan giant anole species are colored blue. Branch lengths are scaled in proportion to nucleotide substitutions and nodes are shaded to indicate Bayesian posterior probability support.

(*b*)

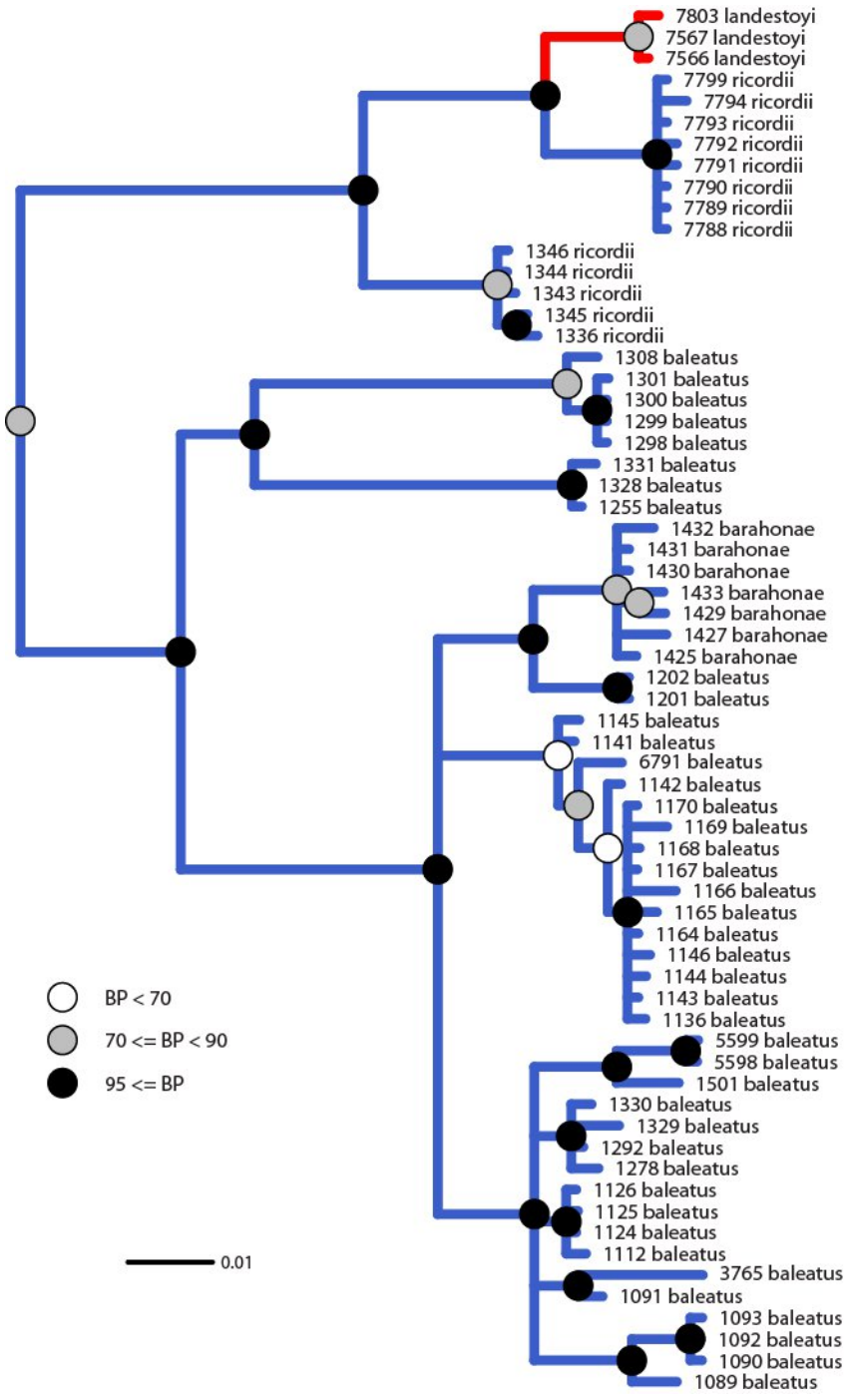

Figure S8 (Continued).

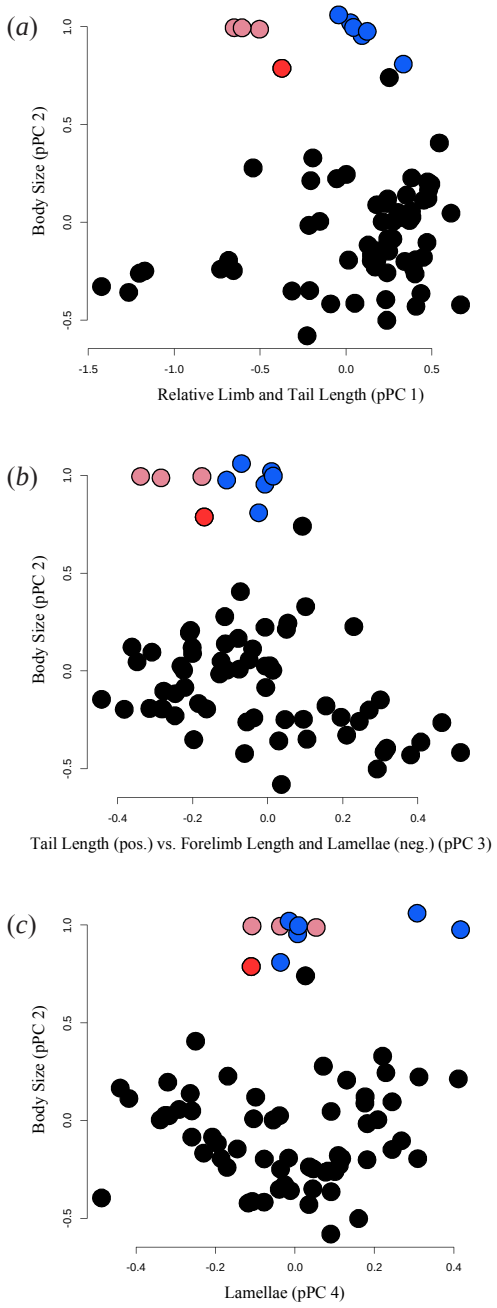

Figure S9. Position of Greater Antillean *Anolis* species in morphospaces defined by body size (pPC 2; y-axis in all plots) and the following shape principal components (x-axis in all plots): (*a*) pPC 1, which correlates positively with limb element lengths and tail length; (*b*) pPC 3, which correlates positively with relative tail length and negatively with forelimb length and toepad lamella number; (*c*) pPC 4, which correlates positively with relative tail length and toepad lamella number and negatively with forelimb length. Colors represent crown-giant anoles (blue), Cuban twig-giant anoles (pink), and *A. landestoyi* sp. nov. (red).

S5: SUPPLEMENTAL LITERATURE CITED

Alföldi, J., F. Di Palma, M. Grabherr, C. Williams, L. Kong, E. Mauceli, P. Russell et al. 2011. The genome of the green anole lizard and a comparative analysis with birds and mammals. Nature 477:587-591.

Ané, C., B. Larget, D. A. Baum, S. D. Smith, and A. Rokas. 2007. Bayesian estimation of concordance among gene trees. Molecular Biology and Evolution 24:412-426.

Beuttell, K., and J. B. Losos. 1999. Ecological morphology of Caribbean anoles. Herpetological Monographs 13:1-28.

Bowersox, S. R., S. Calderón, R. Powell, J. S. Parmerlee Jr., D. D. Smith, and A. Lathrop. 1994. Nahrung eines Riesenanolis, *Anolis barahonae*, von Hispaniola, mit einer Zusammenfassung des Nahrungsspektrums westindischer Riesenanolis-Arten. Salamandra 30:155-160.

Brandley, M. C., A. Schmitz, and T. W. Reeder. 2005. Partitioned Bayesian analyses, partition choice, and the phylogenetic relationships of scincid lizards. Systematic Biology 54:373-390.

Chiari, Y., M. Vences, D. R. Vieites, F. Rabemananjara, P. Bora, O. R. Ravoahangimalala, and A. Meyer. 2004. New evidence for parallel evolution of colour patterns in Malagasy poison frogs (*Mantella*). Molecular Ecology 13:3763-3774.

Chung, Y., and C. Ané. 2011. Comparing two Bayesian methods for gene tree/species tree reconstruction: simulations with incomplete lineage sorting and horizontal gene transfer. Systematic Biology 60:261-275.

Dowling, H. G., and J. M. Savage. 1960. A guide to the snake hemipenis: a survey of basic structure and systematic characteristics. Zoologica: New York Zoological Society 45:17-28.

Drummond, A. J., B. Ashton, S. Buxton, M. Cheung, A. Cooper, C. Duran, M. Field et al. 2010, Geneious v5.3, Available from http://geneious.com.

Drummond, A. J., and A. Rambaut. 2007. BEAST: Bayesian evolutionary analysis by sampling trees. BMC Evolutionary Biology 7:214.

Etheridge, R., and K. de Queiroz. 1988. A phylogeny of Iguanidae, Pages 283-367 *in* R. Estes, and G. Pregill, eds., Phylogenetic Relationships of the Lizard Families: Essays Commemorating Charles L. Camp. Stanford, CA, Stanford University Press.

Glor, R. E., M. E. Gifford, A. Larson, J. B. Losos, L. R. Schettino, A. R. C. Lara, and T. R. Jackman. 2004. Partial island submergence and speciation in an adaptive radiation: a multilocus analysis of the Cuban green anoles. Proceedings of the Royal Society of London B 271:2257-2265.

Glor, R. E., J. J. Kolbe, R. Powell, A. Larson, and J. B. Losos. 2003. Phylogenetic analysis of ecological and morphological diversification in Hispaniolan trunk-ground anoles (*Anolis cybotes* group). Evolution 57:2383-2397.

Heled, J., and A. J. Drummond. 2010. Bayesian inference of species trees from multilocus data. Molecular Biology and Evolution 27:570-580.

Henderson, R. W., and R. Powell. 2009, Natural History of West Indian Reptiles and Amphibians. Gainesville, FL, University Press of Florida.

Hicks, R. A., and R. L. Trivers. 1983. The social behavior of *Anolis valencienni*, Pages 570-595 *in* A. G. J. Rhodin, and K. Miyata, eds., Advances in Herpetology and Evolutionary

Biology: Essays in Honor of Ernest E. Williams. Cambridge, MA, Museum of Comparative Zoology.
Huelsenbeck, J. P., and F. Ronquist. 2001. MRBAYES: Bayesian inference of phylogenetic trees. Bioinformatics 17:754-755.
Larget, B. R., S. K. Kotha, C. N. Dewey, and C. Ané. 2010. BUCKy: Gene tree/species tree reconciliation with Bayesian concordance analysis. Bioinformatics 26:2910-2911.
Leaché, A. D. 2009. Species tree discordance traces to phylogeographic clade boundaries in North American fence lizards (*Sceloporus*). Systematic Biology 58:547-559.
Leaché, A. D., and B. Rannala. 2011. The accuracy of species tree estimation under simulation: A comparison of methods. Systematic Biology 60:126-137.
Losos, J. B. 2009, Lizards in an Evolutionary Tree: Ecology and Adaptive Radiation of Anoles. Berkeley, University of California Press.
Losos, J. B., T. R. Jackman, A. Larson, K. de Queiroz, and L. Rodríguez-Schettino. 1998. Contingency and determinism in replicated adaptive radiations of island lizards. Science 279:2115-2118.
Losos, J. B., M. L. Woolley, D. L. Mahler, O. Torres-Carvajal, K. E. Crandell, E. W. Schaad, A. E. Narváez et al. 2012. Notes on the natural history of the little-known Ecuadorian horned anole, *Anolis proboscis*. Breviora 531:1-17.
Macey, J. R., A. Larson, N. B. Ananjeva, Z. Fang, and T. J. Papenfuss. 1997. Two novel gene orders and the role of light-strand replication in rearrangement of the vertebrate mitochondrial genome. Molecular Biology and Evolution 14:91-104.
Maddison, D. R., and W. P. Maddison. 2005.MacClade 4: Analysis of phylogeny and character evolution. Version 4.08a, version 4.08a.
Maddison, W. P. 1997. Gene trees in species trees. Systematic Biology 46:523-536.
Mahler, D. L., S. M. Lambert, A. J. Geneva, J. Ng, S. B. Hedges, J. B. Losos, and R. E. Glor. 2016. Data from: Discovery of a giant chameleon-like lizard (*Anolis*) on Hispaniola and its significance to understanding replicated adaptive radiations. American Naturalist, Dryad Digital Repository, http://dx.doi.org/10.5061/dryad.sf540.
Mahler, D. L., L. J. Revell, R. E. Glor, and J. B. Losos. 2010. Ecological opportunity and the rate of morphological evolution in the diversification of Greater Antillean anoles. Evolution 64:2731-2745.
Noonan, B. P., and P. T. Chippindale. 2006. Vicariant origin of Malagasy reptiles supports Late Cretaceous Antarctic land bridge. The American Naturalist 168:730-741.
Nylander, J. A. A., J. C. Wilgenbusch, D. L. Warren, and D. L. Swofford. 2008. AWTY (are we there yet?): a system for graphical exploration of MCMC convergence in Bayesian phylogenetics. Bioinformatics 24:581-583.
Paradis, E. 2004. APE: Analyses of Phylogenetics and Evolution in R language. Bioinformatics 20:289-290.
Perdomo, L., Y. Arias, Y. Léon, and D. Wege. 2010, Áreas Importantes para la Conservación de las Aves en la República Dominicana:1-84.
Posada, D. 2008. jModelTest: phylogenetic model averaging. Molecular Biology and Evolution 25:1253-1256.
Posada, D., and K. A. Crandall. 2001. Selecting the best-fit model of nucleotide substitution. Systematic Biology 50:580-601.
Rambaut, A., and A. J. Drummond. 2007, Tracer v1.4, Available from http://beast.bio.ed.ac.uk/Tracer.

Revell, L. J. 2009. Size-correction and principal components for interspecific comparative studies. Evolution 63:3258-3268.

Schwartz, A. 1974. A new species of primitive *Anolis* (Sauria, Iguanidae) from the Sierra de Baoruco, Hispaniola. Breviora 423:1-19.

Swofford, D. L. 2003, PAUP*. Phylogenetic Analysis Using Parsimony (*and Other Methods). Version 4. Sunderland, MA, Sinauer Associates.

Webster, T. P. 1969. Ecological observations on *Anolis occultus* Williams and Rivero (Sauria, Iguanidae). Breviora 312:1-5.

Williams, E. E. 1972. The origin of faunas. Evolution of lizard congeners in a complex island fauna: a trial analysis. Evolutionary Biology 6:47-89.

—. 1983. Ecomorphs, faunas, island size, and diverse end points in island radiations of *Anolis*, Pages 326-370 *in* R. B. Huey, E. R. Pianka, and T. W. Schoener, eds., Lizard Ecology: Studies of a Model Organism. Cambridge, MA, Harvard University Press.

Williams, E. E., and A. S. Rand. 1969. Anolis insolitus, a new dwarf anole of zoogeographic importance from the mountains of the Dominican Republic. Breviora 326:1-21.

Williams, E. E., H. Rand, A. S. Rand, and R. J. O'Hara. 1995. A computer approach to the comparison and identification of species in difficult taxonomic groups. Breviora 502:1-47.